Optimal Neural Compressors for the Rate-Distortion-Perception Tradeoff

Eric Lei[†][*], **Hamed Hassani**[‡], **Shirin Saeedi Bidokhti**[‡]

[†]JPMorganChase Global Technology Applied Research, [‡]University of Pennsylvania
eric.lei@jpmchase.com, {hassani, saeedi}@seas.upenn.edu

Abstract

Recent efforts in neural compression have focused on the rate-distortion-perception (RDP) tradeoff, where the perception constraint ensures the source and reconstruction distributions are close in terms of a statistical divergence. Theoretical work on RDP describes properties of RDP-optimal compressors without providing constructive and low complexity solutions. While classical rate-distortion theory shows that optimal compressors should efficiently pack space, RDP theory additionally shows that infinite randomness shared between the encoder and decoder may be necessary for RDP optimality. In this paper, we propose neural compressors that are low complexity and benefit from high packing efficiency through lattice coding and shared randomness through shared dithering over the lattice cells. For two important settings, namely infinite shared and zero shared randomness, we analyze the RDP tradeoff achieved by our proposed neural compressors and show optimality in both cases. Experimentally, we investigate the roles that these two components of our design, lattice coding and randomness, play in the performance of neural compressors on synthetic and real-world data. We observe that performance improves with more shared randomness and better lattice packing.

1 Introduction

Neural compressors learned from large-scale datasets have achieved state-of-the-art performance in terms of the rate-distortion tradeoff (Ballé et al., 2020; Yang et al., 2023), especially when trained to produce reconstructions that align well with human perception (Mentzer et al., 2020; Tschannen et al., 2018; Agustsson et al., 2019; Muckley et al., 2023). To achieve this, an additional perception loss term is used, typically defined as a statistical divergence δ between the reconstruction and source distributions. As such, recent focus has shifted to the rate-distortion-perception (RDP) framework, where compressors explore a triple tradeoff between rate, distortion and perception δ (Blau and Michaeli, 2019). The RDP function of a source $X \sim P_X$, defined as

$$
\begin{aligned}
R(D, P) = \min_{P_{\hat{X}|X}} \quad & I(X; \hat{X}) \\
\text{s.t.} \quad & \mathbb{E}_{P_X P_{\hat{X}|X}}[\Delta(X, \hat{X})] \leq D, \quad \delta(P_X, P_{\hat{X}}) \leq P,
\end{aligned}
\tag{1}
$$

where Δ is a distortion function, has emerged to describe this fundamental tradeoff (Matsumoto, 2018; Blau and Michaeli, 2019; Li et al., 2011). Several RDP coding theorems have recently been proven (Theis and Wagner, 2021; Wagner, 2022; Chen et al., 2022), providing an operational meaning to (1) as a fundamental limit of lossy compression for the RDP tradeoff[1].

In this paper, we investigate how neural compressors may achieve RDP optimality, and what components are necessary for good RDP performance. The RDP coding theorems, while non-constructive,

---

[*]Prepared prior to employment at JPMorganChase.

[1]Specifically, (1) is achievable by a sequence of source codes, and no source code can do better than (1).
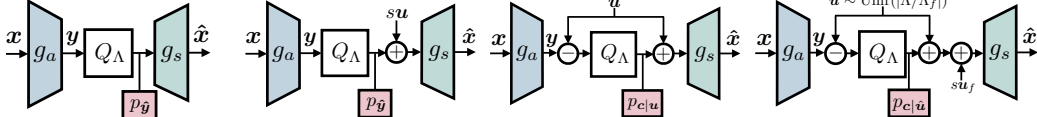
(a) Lattice transform coding (LTC); deterministic.

(b) Private-dither LTC (PD-LTC); $R_c = 0$.

(c) Shared-dither LTC (SD-LTC); $R_c = \infty$.

(d) Quantized-shared-dither LTC (QSD-LTC); finite R_c.

Figure 1: Lattice transform coding (LTC) with R_c bits of (shared) randomness using dithering; $\boldsymbol{u} \sim \mathrm{Unif}(\mathcal{V}_0(\Lambda))$ and $\boldsymbol{u}_f \sim \mathrm{Unif}(\mathcal{V}_0(\Lambda_f))$ are continuous, and $\hat{\boldsymbol{u}} \sim \mathrm{Unif}(|\Lambda/\Lambda_f|)$ is discrete, where Λ, Λ_f are nested lattices. LTC/PD-LTC entropy-code $Q_\Lambda(\boldsymbol{y})$ with likelihoods $p_{\hat{\boldsymbol{y}}}$. SD-LTC and QSD-LTC entropy-code $Q_\Lambda(\boldsymbol{y} - \boldsymbol{u})$ and $Q_\Lambda(\boldsymbol{y} - \hat{\boldsymbol{u}})$ with likelihoods $p_{\boldsymbol{c}|\boldsymbol{u}}$ and $p_{\boldsymbol{c}|\hat{\boldsymbol{u}}}$, respectively.

shed light on properties of RDP-optimal compressors. In contrast to the classical rate-distortion function $R(D) = R(D, \infty)$, which is asymptotically achievable by fully deterministic codes, achieving the RDP function may require not only stochastic encoding/decoding but also *infinite* randomness shared between the encoder and decoder. Devising neural compressors that may achieve RDP optimality at low complexity is an important step in advancing the theory and practice of neural compression. Moreover, infinite shared randomness may not always be available. In settings where shared randomness is *limited*, or *unavailable*, we are still interested in the best possible schemes.

Infinite shared randomness has previously proved successful in RDP-oriented compressors such as Theis et al. (2022) that are based on reverse channel coding (RCC) (Theis and Ahmed, 2022; Li and El Gamal, 2018; Cuff, 2013). RCC enables communication of a sample from a prescribed distribution (e.g., one that is good for RDP) under a limited rate constraint. The performance of RCC is provably near-optimal, but this comes at the cost of high complexity. Moreover, RCC heavily relies on infinite amount of randomness and does not allow for limited or zero randomness. We seek to develop methods with much lower complexity and allow for zero, limited, or infinite amount of randomness.

In the classical rate-distortion framework, recent work has investigated whether neural compressors are optimal, where vector quantization (VQ) (Gersho and Gray, 2012) is known to be optimal, but suffers from high complexity. In Lei et al. (2025), it was shown that lattice transform coding (LTC), which uses lattice quantization (LQ) in the latent space, can achieve performance close to VQ at significantly lower complexity; see also Zhang and Wu (2023); Kudo et al. (2023). VQ and LTC provide near-optimal RD performance due to high space-packing efficiency. However, it is not clear at first glance whether VQ-like coding is good for the RDP setting, where randomized reconstructions are required to satisfy the perception constraint (Tschannen et al., 2018). It is further unclear how randomness should be incorporated with quantization in a way that is RDP-optimal.

Dithering is a common method of randomizing a quantizer. Classically, a shared random dither can help quantization noise admit desired statistical properties, and has applications such as universal quantization (Ziv, 1985), and practical training methods for neural compression (Ballé et al., 2020). For the RDP setting, using dithering to introduce randomness has been investigated recently; Theis and Agustsson (2021) show on a simple source how dithered scalar quantization (SQ) benefits RDP.

In this paper, we introduce randomness, shared and private, into neural compressors via architectures that build on LTC (Fig. 1), and investigate the roles that randomness and quantization play in how neural compressors perform for the RDP tradeoff, while managing complexity. We study LTC where randomness takes the form of a random lattice dither vector. When the randomness is private (i.e., none shared), the dither is only added at the decoder (PD-LTC; Fig. 1b). When the randomness is shared, the dither is subtracted at the encoder, and added back at the decoder (SD-LTC and QSD-LTC; Figs. 1c, 1d respectively). This work unifies transform coding, lattice coding, and randomized coding, identifying the roles each play when used together for RDP. Our contributions are the following[2].

1. We propose LTC with infinite or no shared randomness, using a shared dither (SD-LTC) or private dither (PD-LTC) respectively, and describe the benefits of the former in Sec. 3. We then propose a discrete dithering scheme defined via nested lattices that allows for *finite* randomness to be shared between the encoder and decoder. This scheme, QSD-LTC, interpolates between PD- and SD-LTC, enabling control over the rate of shared randomness.

2. We theoretically analyze and show optimality of SD-LTC and PD-LTC on the Gaussian source with squared 2-Wasserstein perception and asymptotic blocklength in Sec. 4. For the former

---

[2]Code can be found at `https://github.com/leieric/LTC-RDP`.

(where infinite shared randomness is available), we use the sphere-like behavior of lattice cells and the AWGN-like behavior of dithered LQ to show that SD-LTC achieves the RDP function $R(D, P)$. For the latter (where no shared randomness is available), we use lattice Gaussian coding methods to show that under a perception constraint of $P = 0$, PD-LTC achieves $R(D/2, \infty)$, which coincides with the fundamental RDP limit under no shared randomness.

3. We empirically study PD-LTC, SD-LTC, and QSD-LTC performance on synthetic and real-world sources in Sec. 5. We verify our theory and show that RDP performance improves with increased shared randomness and better lattice packing efficiency.

2 Background and Related Work

Neural Compression for RDP. Most neural compressor designs that account for perception are derived from the nonlinear transform coding (NTC) setup (Ballé et al., 2020). These models are parameterized by analysis transform g_a, synthesis transform g_s, and entropy model $p_{\hat{y}}$; see Fig. 1a. To compress a source $\boldsymbol{x}$, the encoder computes the latent $\boldsymbol{y} = g_a(\boldsymbol{x})$, which gets scalar quantized via rounding. The codeword or quantized latent $\hat{\boldsymbol{y}} = Q_\Lambda(\boldsymbol{y})$ is then entropy coded using an entropy model $p_{\hat{y}}$. The decoder provides the reconstruction $\hat{\boldsymbol{x}} = g_s(\hat{\boldsymbol{y}})$. The model is trained end-to-end via

$$\min_\theta \mathbb{E}[-\log p_{\hat{y}}(\hat{\boldsymbol{y}})] + \lambda_1 \mathbb{E}[\Delta(\boldsymbol{x}, \hat{\boldsymbol{x}})] + \lambda_2 \delta(P_{\boldsymbol{x}}, P_{\hat{\boldsymbol{x}}}), \quad (2)$$

where θ denotes the parameters of the codec $(g_a, g_s, p_{\hat{y}})$, and $\lambda_1, \lambda_2 \geq 0$ control the RDP tradeoff. Many state-of-the-art methods (Tschannen et al., 2018; Agustsson et al., 2019; Mentzer et al., 2020; Muckley et al., 2023; He et al., 2022; Zhang et al., 2021) optimize (2), primarily differing in the choice of Δ and the way δ is estimated in practice, which is typically done using an adversarial loss involving a discriminator neural network. The use of randomness (shared or not) in these methods has not always been consistent, nor fully explored in its relation to RDP optimality. While Blau and Michaeli (2019) add uniform noise to the quantized latent, Tschannen et al. (2018); Agustsson et al. (2023) concatenate noise to the quantized latent, and Mentzer et al. (2020); Muckley et al. (2023) do not use randomness at all. Zhang et al. (2021) use (shared) dithered SQ with NTC, but do not explore why or how it is good for RDP. In contrast, we study LQ with dithering under varying levels of shared randomness, and show that one needs both the improved packing efficiency of lattices along with shared lattice dithering to achieve best performance. While there exist a few RDP-oriented neural compressors that do not fit the NTC framework (Theis et al., 2022; Yang et al., 2024; Yang and Mandt, 2024) and instead leverage diffusion models, our work focuses on NTC-style neural compressors for RDP, as they remain the most pervasive type of neural compressor in use, and do not suffer from the higher complexity of RCC or diffusion models.

Information-Theoretic Analysis of RDP. The RDP function in (1) was formally introduced and widely adopted following Blau and Michaeli (2019); see also earlier related work by Matsumoto (2018); Li et al. (2011); Saldi et al. (2015). (1) is a purely informational quantity, i.e., a function of the source P_X, and thus does not have a meaning as a fundamental limit of compression without a corresponding coding theorem describing it as such. The first RDP coding theorem was provided by Saldi et al. (2015), who show that for perfect perception ($P = 0$), (1) is achievable under infinite shared randomness, and conversely that no compressor can outperform (1). For general P, Theis and Wagner (2021) establish optimality (i.e., achievability and converse) of (1) when infinite shared randomness is available. Saldi et al. (2015) further characterize the fundamental RDP limit at $P = 0$ when only R_c bits per sample of shared randomness is allowed, which only coincides with (1) when $R_c = \infty$; a smaller R_c results in a strictly worse fundamental limit (see also Wagner (2022)). This establishes the necessity of infinite shared randomness to achieve (1). Li et al. (2011) use dithered LQ to show achievability of (1) for $P = 0$; in contrast, we show this to be true for general P and also analyze the $R_c = 0$ case, which requires a new set of proof techniques based on lattice Gaussian coding (Ling and Belfiore, 2014). Under private randomness ($R_c = 0$), Yan et al. (2021) establish $R(D/2, \infty)$ as the fundamental limit for $P = 0$; Hamdi et al. (2024a) show that randomized encoders do not help. Chen et al. (2022) study the RDP tradeoff when the perception constraint is strong- or weak-sense[3]. Under weak-sense, it was shown that $R(D, P)$ is achievable without shared randomness, whereas under strong-sense, shared randomness is necessary, agreeing with Saldi et al. (2015); Wagner (2022). In our work, we focus on strong-sense, since that is typically how the

---

[3]On vectors $\boldsymbol{x}, \hat{\boldsymbol{x}} \in \mathbb{R}^n$, strong-sense denotes $\delta(P_{\boldsymbol{x}}, P_{\hat{\boldsymbol{x}}}) < P$; weak-sense denotes $\delta(P_{\boldsymbol{x}_i}, P_{\hat{\boldsymbol{x}}_i}) < P, \forall i$.

perception is measured in practice (i.e., in (2)). In particular, we focus on strong-sense Wasserstein, since that aligns with δ's and evaluation metrics chosen in practice such as Fréchet inception distance.

Coding theorems use schemes that are typically not constructive (e.g., random coding) and/or not practical (e.g., high complexity RCC schemes). They do, however, provide insights on structures that may be useful or even necessary for optimality. In addition to the necessity of infinite shared randomness to achieve (1), we show in Sec. A how the RCC scheme of Theis and Wagner (2021) implies that a good RDP compressor should behave like a randomized VQ: it should have VQ-like packing efficiency (i.e., good for distortion) combined with random codewords that follow the right distribution (i.e, good for perception). In our work, the former is handled with LQ (at low complexity), while the latter is handled with dithering; our schemes are further shown optimal on Gaussians.

The benefits of (potentially shared) randomness have also been discussed outside the context of coding theorems. Tschannen et al. (2018) show how randomized decoders are necessary to achieve perfect perceptual quality. Theis and Agustsson (2021) illustrate how quantizers benefit from shared randomness on a toy circle source. Similarly, Zhou and Tian (2024) demonstrate how staggered SQ can use limited shared randomness to improve performance on the circle. In contrast, our work presents a more general approach for infinite, limited, and no shared randomness with LQ that empirically shows its benefits and is provably optimal on Gaussians.

Lattice Quantization. Lattice quantization (LQ) involves a lattice Λ, which consists of a countably infinite set of codebook vectors in n-dimensional space (Conway and Sloane, 1999; Zamir et al., 2014). We denote $Q_\Lambda(\boldsymbol{x}) := \arg\min_{\boldsymbol{\lambda} \in \Lambda} \|\boldsymbol{\lambda} - \boldsymbol{x}\|^2$ as the LQ of a vector $\boldsymbol{x} \in \mathbb{R}^n$. The fundamental cell, or Voronoi region, of the lattice is given by $\mathcal{V}_0(\Lambda) := \{\boldsymbol{x} \in \mathbb{R}^n : Q_\Lambda(\boldsymbol{x}) = \boldsymbol{0}\}$, i.e., the set of all vectors quantized to $\boldsymbol{0}$. We denote the lattice volume as $V(\Lambda) := \int_{\mathcal{V}_0(\Lambda)} d\boldsymbol{x}$, the lattice second moment as $\sigma^2(\Lambda) := \frac{1}{n} \mathbb{E}_{\boldsymbol{u} \sim \mathrm{Unif}(\mathcal{V}_0(\Lambda))}[\|\boldsymbol{u}\|^2]$, and the normalized second moment (NSM) $G(\Lambda) = \frac{\sigma^2(\Lambda)}{(V(\Lambda))^{2/n}}$. The lattice's packing efficiency can be measured by how small its NSM is; it is known that there exists sequences of lattices $\{\Lambda^{(n)}\}_{n=1}^\infty$ that achieve the sphere lower bound, i.e., $\lim_{n \to \infty} G(\Lambda^{(n)}) = \frac{1}{2\pi e}$, where the lattice cells become sphere-like (Zamir et al., 2014, Ch. 7). The closest vector problem (CVP), which finds $Q_\Lambda(\boldsymbol{x})$, is NP-hard in general, but many lattices with low NSM (e.g., E_8, Barnes-Wall, Leech) have efficient CVP solvers. Recently proposed polar lattices (Liu et al., 2021), which have polynomial time CVP, were shown to be sphere-bound-achieving (Liu et al., 2024). Recently, LQ was explored in neural compression (Zhang and Wu, 2023; Kudo et al., 2023) as a low-complexity method that improves the poor packing efficiency of SQ, equivalent to the integer lattice $\mathbb{Z}_n$. Lei et al. (2025) showed that NTC transforms are insufficient to overcome the poor packing efficiency of a suboptimal lattice, leading to the lattice transform coding (LTC) framework; performance improves with increased lattice packing efficiency.

3 Lattice Transform Coding for RDP

We seek to design compressors that are RDP-optimal given constraints on the amount of shared randomness available and are also low complexity. As mentioned in Sec. 2, we show in Sec. A that a good RDP scheme should implement randomized VQ. Dithering is a method that can enable a quantizer to be randomized. In the context of neural compression, NTC transforms are unable to generate VQ-like regions in the source space due to the limited packing efficiency of latent space SQ (Lei et al., 2025). The LTC framework, which uses latent LQ, can provide the benefits of VQ-like regions in the source space. LQ naturally supports dithering that is uniform over the lattice cell. Thus, dithered LQ emerges as a promising scheme that is both randomized and VQ-like, while maintaining low complexity. In the following, we describe how LQ with dithering can be integrated into the LTC framework and trained end-to-end. We present three architectures that handle the cases of infinite-, no-, and finite-shared randomness via a shared-, private-, and quantized shared-dither, respectively.

3.1 LTC with Infinite Shared Randomness

We first define the shared-dither LTC, which assumes infinite shared randomness is available between the encoder and decoder. We denote the fundamental cell $\mathcal{V}_0(\Lambda)$ as $\mathcal{V}_0$ for ease of notation.

Definition 3.1 (Shared-Dither Lattice Transform Code (SD-LTC); Fig. 1c). A SD-LTC is a triple (g_a, g_s, Λ), with mappings g_a, g_s and lattice Λ. A random dither $\boldsymbol{u} \sim \mathrm{Unif}(\mathcal{V}_0(\Lambda))$, uniform over the

lattice cell, is shared between the encoder and decoder. The SD-LTC computes the latent $\boldsymbol{y} = g_a(\boldsymbol{x})$, entropy codes $\boldsymbol{c} = Q_\Lambda(\boldsymbol{y} - \boldsymbol{u})$ at the encoder, and the decoder outputs $\hat{\boldsymbol{x}} = g_s(\boldsymbol{c} + \boldsymbol{u})$.

Since $\boldsymbol{u}$ is available at the encoder and decoder (which utilizes the availability of infinite shared randomness), the operational rate of SD-LTC is given by

$$H(\boldsymbol{c}|\boldsymbol{u}) = \mathbb{E}_{\boldsymbol{y},\boldsymbol{u}}[-\log p_{\boldsymbol{c}|\boldsymbol{u}}(\boldsymbol{c}|\boldsymbol{u}))] = \mathbb{E}_{\boldsymbol{y},\boldsymbol{u}}\left[-\log \int_{\mathcal{V}_0+\boldsymbol{c}} p_{\boldsymbol{y}-\boldsymbol{u}|\boldsymbol{u}}(\boldsymbol{w}|\boldsymbol{u})d\boldsymbol{w}\right] \tag{3}$$

$$= \mathbb{E}_{\boldsymbol{y},\boldsymbol{u}}[-\log \mathbb{E}_{\boldsymbol{u}'}[p_{\boldsymbol{y}}(Q_\Lambda(\boldsymbol{y} - \boldsymbol{u}) + \boldsymbol{u} + \boldsymbol{u}')]], \tag{4}$$

where $\boldsymbol{u}' \sim \mathrm{Unif}(\mathcal{V}_0)$. As an alternative, we can make use of the additive channel equivalence $(Q_\Lambda(\boldsymbol{y} - \boldsymbol{u}) + \boldsymbol{u} \overset{d}{=} \boldsymbol{y} + \boldsymbol{u}_{\mathrm{eq}}$, where $\boldsymbol{u}_{\mathrm{eq}} \sim \mathrm{Unif}(\mathcal{V}_0(\Lambda)))$ (Zamir et al., 2014, Thm. 5.2.1), yielding

$$H(\boldsymbol{c}|\boldsymbol{u}) = I(\boldsymbol{y}; \boldsymbol{y} + \boldsymbol{u}) = h(\boldsymbol{y} + \boldsymbol{u}) - h(\boldsymbol{u}) = \mathbb{E}_{\boldsymbol{y},\boldsymbol{u}}[-\log p_{\boldsymbol{y}+\boldsymbol{u}}(\boldsymbol{y} + \boldsymbol{u})] - \log V(\Lambda) \tag{5}$$

$$= \mathbb{E}_{\boldsymbol{y},\boldsymbol{u}}\left[-\log \int_{\mathcal{V}_0(\Lambda)+\boldsymbol{y}+\boldsymbol{u}} p_{\boldsymbol{y}}(\boldsymbol{w})d\boldsymbol{w}\right] = \mathbb{E}_{\boldsymbol{y},\boldsymbol{u}}[-\log \mathbb{E}_{\boldsymbol{u}'}[p_{\boldsymbol{y}}(\boldsymbol{y} + \boldsymbol{u} + \boldsymbol{u}')]], \tag{6}$$

where $h(\cdot)$ denotes differential entropy, $V(\Lambda)$ is the lattice volume, and (6) holds since $p_{\boldsymbol{y}+\boldsymbol{u}}(\boldsymbol{y} + \boldsymbol{u}) = \frac{1}{V(\Lambda)} \int_{\mathcal{V}_0(\Lambda)+\boldsymbol{y}+\boldsymbol{u}} p_{\boldsymbol{y}}(\boldsymbol{w})d\boldsymbol{w}$. The objective is trained with $\min_\theta H(\boldsymbol{c}|\boldsymbol{u}) + \lambda_1 \mathbb{E}[\Delta(\boldsymbol{x}, \hat{\boldsymbol{x}})] + \lambda_2 \delta(P_{\boldsymbol{x}}, P_{\hat{\boldsymbol{x}}})$, with learned parameters θ. Either (4) or (6) can be used for $H(\boldsymbol{c}|\boldsymbol{u})$; (4) requires the straight-through estimator due to non-differentiability of the quantizer. In the following, we comment on several connections between (4), (6), and other work in the neural compression literature.

Integrating the learned $p_{\boldsymbol{y}}$. The inner integral in (4) and (6) can be computed exactly under SQ (equivalently, $\Lambda = \mathbb{Z}^n$) using the CDF of $p_{\boldsymbol{y}}$, following Ballé et al. (2018). For general lattices, the inner integral can be estimated using Monte-Carlo following Lei et al. (2025), by sampling vectors uniform over the lattice cell (Conway and Sloane, 1984).

Noisy proxies and operational rates. The equivalence of (4) and (6) was shown in Ballé et al. (2020) for $\Lambda = \mathbb{Z}_n$. Their equivalence for general lattices, as shown above, follows from Zamir et al. (2014). Ballé et al. (2020) uses this equivalence to support (6) as a training objective, which is known as the noisy proxy to quantization in the literature. This is useful since (6) is differentiable with respect to $\boldsymbol{y}$, whereas (4) is not. Here, we emphasize that both (4) and (6) represent the operational rate for a SD-LTC. For deterministic NTC/LTC trained with the noisy proxy, a deterministic dither (perhaps $\boldsymbol{0}$) is chosen test time, resulting in a different operational rate that does not average over $\boldsymbol{u}$. Agustsson and Theis (2020) proposed dithered SQ as universal quantization; however, they were motivated by reducing train/test rate mismatch rather than the RDP tradeoff, which is the focus of our work.

3.2 LTC with No Shared Randomness

We now consider when no shared randomness is available. As mentioned, decoder randomness is needed for the perception constraint, and this manifests itself as a private dither at the decoder.

Definition 3.2 (Private-Dither Lattice Transform Code (PD-LTC); Fig. 1b). A PD-LTC is a triple (g_a, g_s, Λ), with transforms g_a and g_s and lattice Λ. A random dither $\boldsymbol{u} \sim \mathrm{Unif}(\mathcal{V}_0(\Lambda))$, uniform over the lattice cell, is at the decoder only. The PD-LTC entropy-codes $\hat{\boldsymbol{y}} = Q_\Lambda(g_a(\boldsymbol{x}))$, and the decoder outputs $\hat{\boldsymbol{x}} = g_s(\hat{\boldsymbol{y}} + s\boldsymbol{u})$, where $s > 0$ is a parameter that controls the dither magnitude.

For a PD-LTC (shown in Fig. 1b), the operational rate is the same as in deterministic LTC, given by $H(\hat{\boldsymbol{y}}) = \mathbb{E}_{\boldsymbol{y}}[-\log p_{\hat{\boldsymbol{y}}}(\hat{\boldsymbol{y}})]$, as there is no shared dither. Therefore, the training objective remains the same as (2). The following proposition provides some intuition on why shared-dither quantization (Fig. 1c) is superior to private-dither quantization (Fig. 1b) in terms of distortion.

Proposition 3.3. *Define* $\hat{\boldsymbol{x}}_{\mathsf{SD}} = Q_\Lambda(\boldsymbol{x} - \boldsymbol{u}) + \boldsymbol{u}$, $\hat{\boldsymbol{x}}_{\mathsf{PD}} = Q_\Lambda(\boldsymbol{x}) + s\boldsymbol{u}$. *For any* $\boldsymbol{x}$ *and* $s \geq 1$,

$$\mathbb{E}\big[\|\boldsymbol{x} - \hat{\boldsymbol{x}}_{\mathsf{PD}}\|^2\big] = s^2 \, \mathbb{E}\big[\|\boldsymbol{x} - \hat{\boldsymbol{x}}_{\mathsf{SD}}\|^2\big] + \mathbb{E}\big[\|\boldsymbol{x} - Q_\Lambda(\boldsymbol{x})\|^2\big] \geq \mathbb{E}\big[\|\boldsymbol{x} - \hat{\boldsymbol{x}}_{\mathsf{SD}}\|^2\big]. \tag{7}$$

The proof is provided in Sec. D; note that $\boldsymbol{x}$ here is an arbitrary vector (not necessarily the source). Prop. 3.3 implies the PD error is the sum of the SD error and the error under deterministic quantization; see Fig. 2. While $\hat{\boldsymbol{x}}_{\mathsf{SD}}$ is random over the blue cell, incurring error equal to the lattice second moment, $\hat{\boldsymbol{x}}_{\mathsf{PD}}$ is random over the gray cell, incurring additional quantization error. Regarding $s \geq 1$, lower PD error is possible with $s < 1$, but the support of $\hat{\boldsymbol{y}} + s\boldsymbol{u}$ would have gaps within each lattice cell, which may make the perception constraint difficult to satisfy. In Sec. 4, we show that $s > 1$ is necessary for PD-LTC to achieve optimality on the Gaussian source.

While Prop. 3.3 provides an idea of how SD-LTC and PD-LTC may perform distortion-wise, the rate and perception are more complicated. For perception, the induced reconstruction distributions are different, since that of $\hat{x}_{\text{SD}}$ is a convolution between the source and a zero-mean dither, whereas that of $\hat{x}_{\text{PD}}$ is a mixture of dithers centered on lattice vectors. For the rate, compared to $H(\hat{y})$, $H(c|u)$ has additional randomness due to the averaging over u, and thus we may expect the rate of SD-LTC to be larger than that of PD-LTC if they share the same transforms. Ideally, this potential increase in rate can help achieve an overall superior RDP tradeoff for SD-LTC. In Sec. 4, we show that this is true on the Gaussian source, and verify it empirically on real-world sources as well in Sec. 5.
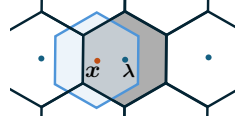

Figure 2: Reconstr. of x under PD (gray) or SD (blue); $s = 1$.

3.3 LTC with Finite Shared Randomness

While the availability of truly infinite shared randomness may be difficult to obtain in practice, the availability of finite shared randomness may be more feasible. Let R_c denote the rate of shared randomness in bits per dimension. RDP theory informs us that performance should improve as R_c increases (Sec. 2). To make use of finite shared randomness, we propose a scheme (Fig. 1d) that interpolates between SD-LTC and PD-LTC by using nested lattices (Zamir et al., 2014, Ch. 8). Lattices Λ, Λ_f are nested if Λ is a sub-lattice of the fine lattice Λ_f. We restrict our attention to self-similar nested lattices $\Lambda = a\Lambda_f$ where $a > 0$ is an integer. We denote $\Lambda/\Lambda_f = \{\boldsymbol{\lambda} \in \Lambda_f : \boldsymbol{\lambda} \in \mathcal{V}_0(\Lambda)\}$ as the fine lattice vectors contained in the fundamental cell of Λ.

Definition 3.4 (Quantized Shared-Dither Lattice Transform Code (QSD-LTC); Fig. 1d)**.** A QSD-LTC is given by $(g_a, g_s, \Lambda, \Lambda_f)$, with mappings g_a, g_s and nested lattices Λ, Λ_f. A random discrete dither $\hat{u} \sim \text{Unif}(\Lambda/\Lambda_f)$ is shared between the encoder and decoder, and a continuous dither $u_f \sim \text{Unif}(\mathcal{V}_0(\Lambda_f))$ uniform over Λ_f's cell is at the decoder only. The QSD-LTC computes $y = g_a(x)$, entropy codes $c = Q_\Lambda(y - \hat{u})$, and the decoder outputs $\hat{x} = g_s(c + \hat{u} + su_f)$. The rate of shared randomness is $R_c = \frac{1}{n}\log|\Lambda/\Lambda_f|$ bits, i.e., there are 2^{nR_c} possible shared dither vectors.

Remark 3.5. QSD-LTC recovers PD-LTC and SD-LTC when $R_c = 0$ and $R_c = \infty$, respectively:

- When $R_c = 0$, we have that $\Lambda_f = \Lambda$, $\hat{u} = \mathbf{0}$, and $u_f \sim \text{Unif}(\mathcal{V}_0(\Lambda))$, and therefore
$$Q_\Lambda(y - \hat{u}) + \hat{u} + su_f = Q_\Lambda(y) + su_f. \tag{8}$$
- When $R_c = \infty$, we have that $\Lambda_f = \mathbb{R}^n$, $\hat{u} \sim \text{Unif}(\mathcal{V}_0(\Lambda))$, $u_f = \mathbf{0}$, and therefore
$$Q_\Lambda(y - \hat{u}) + \hat{u} + su_f = Q_\Lambda(y - \hat{u}) + \hat{u}. \tag{9}$$

The operational rate, $H(c|\hat{u})$, follows (4), except replacing u with $\hat{u}$. The training objective is $\min_\theta H(c|\hat{u}) + \lambda_1 \mathbb{E}[\Delta(x, \hat{x})] + \lambda_2 \delta(P_x, P_{\hat{x}})$. Unlike SD-LTC, the additive channel equivalence does not apply, since the support of $y - \hat{u} - Q_\Lambda(y - \hat{u})$ is random and does not always equal Λ/Λ_f.

We note that the R_c values that QSD-LTC may achieve are limited to $\log\Gamma$, where $\Gamma \in \mathbb{Z}^+$, a positive integer, is the nesting ratio of Λ, Λ_f (Zamir et al., 2014, Ch. 8). This is due to the structure of nested lattices. To achieve R_c values between 0 and 1, a non-uniform distribution for the shared dither vector $\hat{u}$ would need to be employed; we leave this to future work.

Remark 3.6. One may ask whether infinite shared randomness can be obtained by sending a pseudorandom seed and drawing continuous dither vectors $u \sim \text{Unif}(\mathcal{V}_0(\Lambda))$ from a random number generator (RNG) based on the seed. If one compresses a source realization x to a bitstream b, a pseudorandom seed of k bits would imply that only 2^k possible dither vectors could be used at the decoder to decode b; this is noted by Hamdi et al. (2024b). Therefore, sending a pseudorandom seed is insufficient to simulate infinite shared randomness; rather, it implements a scheme with finite shared randomness. Furthermore, finite shared randomness with a constant number of bits *per dimension* is necessary to achieve the fundamental limits (Wagner, 2022); this is impossible to satisfy with a random seed of a fixed number of k bits for high-dimensional sources. In addition to having the capability of imposing a R_c bits per dimension of shared randomness, QSD-LTC has the additional advantage of ensuring the dither vectors are drawn uniformly from the fine lattice vectors in the lattice cell $\mathcal{V}_0(\Lambda)$. These are spread out uniformly throughout $\mathcal{V}_0(\Lambda)$ due to the structure of nested lattices. In comparison, dither vectors drawn from a random seed have no guarantee on where they may land in $\mathcal{V}_0(\Lambda)$, and would depend on the RNG and seed used. As an example, for a poorly chosen seed and RNG, the dither vectors generated could all be concentrated near the center of $\mathcal{V}_0(\Lambda)$, which would effectively yield no shared randomness. Therefore, in settings where infinite shared randomness is impractical, QSD-LTC enables a structured way of using finite shared randomness.

6

On complexity. SD-, PD-, and QSD-LTC rely on LQ. For a fixed lattice up to dimension 24 (Sec. 2), the closest codebook vector search (also used to generate dithers) can be performed at any rate in a fixed number of operations, and is significantly faster than that of VQ, which is exponential in the rate. For higher dimensions, polar lattices have complexity polynomial in the dimension.

4 Achieving the Fundamental Limits

We now theoretically analyze the performance of SD-LTC and PD-LTC on the Gaussian source, and describe the RDP tradeoff asymptotically achievable by SD-LTC and PD-LTC. While the operational rate and distortion are given by the per-dimension versions of those in Sec. 3, the operational perception used is per-dimension squared 2-Wasserstein distance. We leave full proofs to Sec. D.

4.1 Infinite Shared Randomness

Proposition 4.1 (RDP function for Gaussian source (Zhang et al., 2021)). *Let $P_X = \mathcal{N}(0, \sigma^2)$, $\Delta(x, \hat{x}) = (x - \hat{x})^2$, and $\delta(\mu, \nu) = W_2^2(\mu, \nu)$ be squared 2-Wasserstein distance. Then*

$$R(D, P) = \begin{cases} \frac{1}{2} \log \frac{\sigma^2 (\sigma - \sqrt{P})^2}{\sigma^2 (\sigma - \sqrt{P})^2 - \left(\frac{\sigma^2 + (\sigma - \sqrt{P})^2 - D}{2}\right)^2}, & \text{for } \sqrt{P} < \sigma - \sqrt{|\sigma^2 - D|}, \\ \max\left\{\frac{1}{2} \log \frac{\sigma^2}{D}, 0\right\}, & \text{for } \sqrt{P} \geq \sigma - \sqrt{|\sigma^2 - D|}. \end{cases} \tag{10}$$

Remark 4.2. When $\sqrt{P} < \sigma - \sqrt{|\sigma^2 - D|}$, the optimal $\hat{X}$ in (1) is jointly Gaussian with marginal $\hat{X} \sim \mathcal{N}(0, (\sigma - \sqrt{P})^2)$, and covariance $\theta = \max\left\{\frac{1}{2}(\sigma^2 + (\sigma - \sqrt{P})^2 - D), 0\right\}$. When $\sqrt{P} \geq \sigma - \sqrt{|\sigma^2 - D|}$, $\hat{X}$ is jointly Gaussian with marginal $\hat{X} \sim \mathcal{N}(0, \sigma^2 - D)$.

The following theorem shows that $R(D, P)$ is achievable with SD-LTCs, and is an extension of Li et al. (2011), whose authors addressed the $P = 0$ case.

Theorem 4.3 (Optimality of SD-LTC for Gaussian source). *Let $X_1, X_2, \ldots \overset{\text{i.i.d.}}{\sim} \mathcal{N}(0, \sigma^2)$. For any $P \in [0, \sigma^2], D \in [0, 2\sigma^2]$, there exists a sequence of SD-LTCs $\{(g_a^{(n)}, g_s^{(n)}, \Lambda^{(n)})\}_{n=1}^{\infty}$ such that*

$$\lim_{n \to \infty} \frac{1}{n} H(Q_{\Lambda^{(n)}}(g_a^{(n)}(X^n) - \boldsymbol{u}) | \boldsymbol{u}) = R(D, P), \tag{11}$$

$$\lim_{n \to \infty} \frac{1}{n} \mathbb{E}\left[\|X^n - \hat{X}^n\|_2^2\right] \leq D, \tag{12}$$

$$\lim_{n \to \infty} \frac{1}{n} W_2^2(P_{X^n}, P_{\hat{X}^n}) \leq P, \tag{13}$$

where $\hat{X}^n = g_s^{(n)}(Q_{\Lambda^{(n)}}(g_a^{(n)}(X^n) - \boldsymbol{u}) + \boldsymbol{u})$, and $\boldsymbol{u} \sim \text{Unif}(\mathcal{V}_0(\Lambda^{(n)}))$.

Remark 4.4. The proof of Thm. 4.3 relies on a sphere-bound-achieving sequence of lattices with scalar transforms g_a, g_s. As dimension grows, the dither $\boldsymbol{u}$ becomes Gaussian-like, and the latent dithered LQ acts like an additive Gaussian channel (Zamir and Feder, 1996), imposing a joint Gaussian relationship between X and $\hat{X}$ as desired by the RDP solution; see Remark 4.2 and Fig. 3.

4.2 No Shared Randomness

We now consider the case when the encoder and decoder do not have access to any shared randomness. For simplicity and ease of presentation, we consider the regime of near-perfect and perfect perception, corresponding to $P < \epsilon$ for any $\epsilon > 0$ and $P = 0$, respectively. This is the only regime of perception where lower bounds on the RDP achievable under no shared randomness are known (Saldi et al., 2015; Wagner, 2022; Chen et al., 2022; Yan et al., 2021), which corresponds to $R(D/2, \infty)$, and evaluates to $\frac{1}{2} \log \frac{2\sigma^2}{D}$ on the i.i.d. Gaussian source. The following theorem shows that $R(D/2, \infty)$ is achievable with PD-LTCs under near-perfect perception, which can be easily extended to perfect perception (see Remark D.8). As discussed in Sec. 2, $R(D, 0) < R(D/2, \infty)$; see Fig. 4 for a visualization.
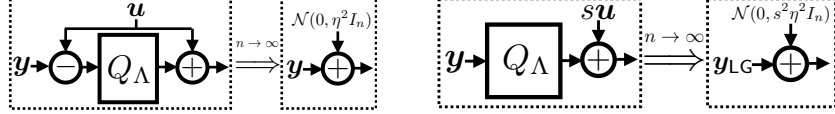
Figure 3: In the latent space, SD-LTC (left) becomes AWGN-like. PD-LTC (right) models the sum of a lattice Gaussian and Gaussian; s must be large enough for the sum to be Gaussian.

Theorem 4.5 (Optimality of PD-LTC for Gaussian source). *Let $X_1, X_2, \ldots \overset{\text{i.i.d.}}{\sim} \mathcal{N}(0, \sigma^2)$. For any D satisfying $0 < D \leq 2\sigma^2$, there exists a sequence of PD-LTCs $\{(g_a^{(n)}, g_s^{(n)}, \Lambda^{(n)})\}_{n=1}^{\infty}$ such that*

$$\lim_{n \to \infty} \frac{1}{n} H(Q_{\Lambda^{(n)}}(g_a^{(n)}(X^n))) \leq R(D/2, \infty), \tag{14}$$

$$\lim_{n \to \infty} \frac{1}{n} \mathbb{E}[\|X^n - \hat{X}^n\|^2] \leq D, \tag{15}$$

$$\lim_{n \to \infty} \frac{1}{n} W_2^2(P_{X^n}, P_{\hat{X}^n}) = 0, \tag{16}$$

where $\hat{X}^n = g_s^{(n)}(Q_{\Lambda^{(n)}}(g_a^{(n)}(X^n)) + s\boldsymbol{u})$, $\boldsymbol{u} \sim \text{Unif}(\mathcal{V}(\Lambda^{(n)}))$, and $s = \frac{\sigma}{\sqrt{\sigma^2 - D/2}}$.

Remark 4.6. PD-LTC does not use a shared dither; we cannot make use of classical results (Zamir and Feder, 1996) to analyze the statistical behavior of latent LQ as an additive channel (as opposed to Thm. 4.3). Instead, Thm. 4.5 relies on lattice Gaussian coding methods (Ling and Belfiore, 2014); see Sec. D.3 for details. Using scalar transforms, $Q_\Lambda(g_a(\boldsymbol{x}))$ behaves like a lattice Gaussian. The additive private dither $s\boldsymbol{u}$ (which becomes Gaussian-like) makes the reconstruction Gaussian-like (Fig. 3). It then suffices for g_s to scale $\hat{X}^n$ to impose the desired variance σ^2. In classical rate-distortion, dithered LQ and lattice Gaussian coding can both achieve optimality, so their differences are primarily practical (e.g., restrictions on lattice families, availability of a shared dither). Thms. 4.3, 4.5 show that with a perception constraint, the two proof techniques lead to different fundamental limits as well.

Remark 4.7. We note that the choice of $s = \sigma/\sqrt{\sigma^2 - D/2} > 1$ depends on the regime of the rate-distortion tradeoff; it is approximately 1 for small D, and becomes large for $D \to 2\sigma^2$. At low rates, this means the effective dither $s\boldsymbol{u}$ "leaks" outside the lattice cell rather significantly. This is required to ensure the perception term vanishes in (16). Specifically, $s\boldsymbol{u}$ needs to be large enough relative to the quantization steps of $Q(g_a^{(n)}(X^n))$ for $Q_{\Lambda^{(n)}}(g_a^{(n)}(X^n)) + s\boldsymbol{u}$ to approximate a Gaussian of covariance $\sigma^2 I_n$ arbitrarily accurately. The nature of this approximation is based on the flatness factor (Ling et al., 2014, Def. 5) used in lattice Gaussian coding, which is elaborated on in Remark D.7.

5 Experimental Results

Experimental setup. We denote n the source dimension and n_L the latent space dimension. We denote LTC as NTC when the lattice is chosen to be the integer lattice, i.e., $\Lambda = \mathbb{Z}_{n_L}$. We train the PD-, SD- and QSD-LTC models using their RDP objectives discussed in Sec. 3. For the rates reported at test time, we use the (4) version of $H(\boldsymbol{c}|\boldsymbol{u})$ for SD-LTC, $\mathbb{E}_{\boldsymbol{y}}[-\log p_{\hat{\boldsymbol{y}}}(\hat{\boldsymbol{y}})]$ for PD-LTC, and $H(\boldsymbol{c}|\hat{\boldsymbol{u}})$ for QSD-LTC; all require hard quantization. These rates are cross-entropy upper bounds on the true entropy, due to the learned $p_{\boldsymbol{y}}$ density. We use MSE distortion $\Delta(\boldsymbol{x}, \hat{\boldsymbol{x}}) = \frac{1}{n}\|\boldsymbol{x} - \hat{\boldsymbol{x}}\|_2^2$.

Figure 4: Effect of lattice choice and shared randomness on Gaussians at $P = 0$.

For perception, to obtain reliable estimates in higher dimensions, we use squared sliced Wasserstein distance (Bonneel et al., 2015) of order 2, $\delta(P_{\boldsymbol{x}}, P_{\hat{\boldsymbol{x}}}) = \frac{1}{n}\text{SW}_2^2(P_{\boldsymbol{x}}, P_{\hat{\boldsymbol{x}}})$. During training, we use the straight-through estimator with hard quantization. See Sec. B for further details on architecture/training.
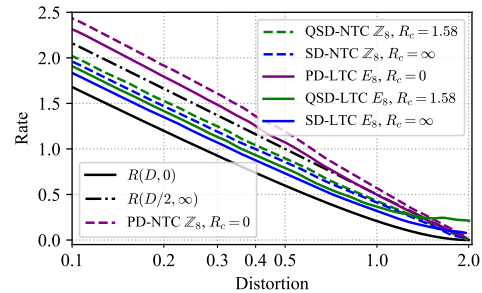
5.1 Synthetic Sources

We first evaluate the i.i.d. Gaussian source of dimension $n = 8$. In Fig. 4, we plot the equi-perception curves with $P = 0$ to compare the methods under the perfect realism setting. As shown, for a fixed
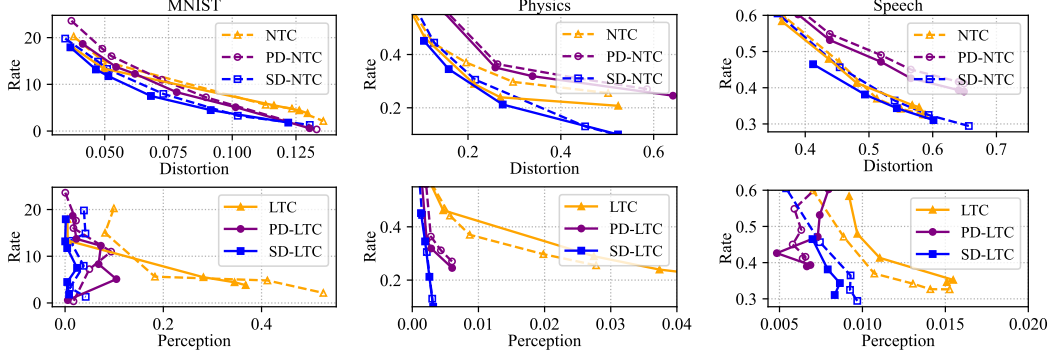
Figure 5: LTC, PD-LTC, and SD-LTC on real-world sources; R-D (top) and R-P (bottom).
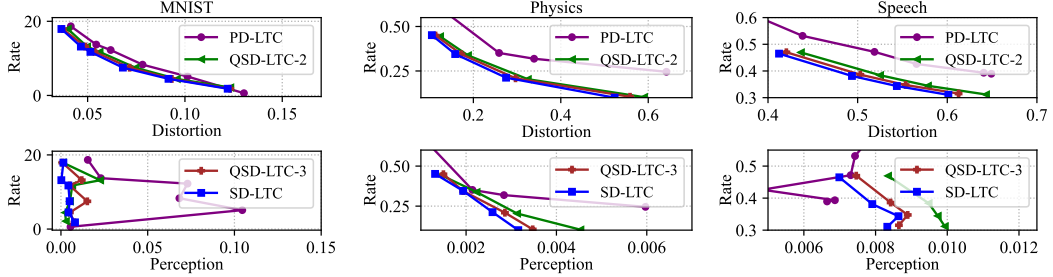

Figure 6: QSD-LTC-Γ (Γ the nesting ratio) on real-world sources; R-D (top) and R-P (bottom).

amount of shared randomness, a more efficient lattice improves performance. Analogously, for a fixed lattice, more shared randomness improves performance. We additionally evaluate QSD-LTC with finite shared randomness. The fine lattice Λ_f in Def. 3.4 is set to be self-similar with Λ, with a nesting ratio of 3. This results in $R_c = \log 3$ bits per dimension. As shown, the QSD-LTC performance is nearly able to achieve that of SD-LTC, despite not having infinite shared randomness; this verifies that QSD-LTC allows one to interpolate between SD-LTC and PD-LTC. At low rates, the LTC with E_8 has some suboptimality; this is due to the Monte-Carlo estimation when computing the integral for latent likelihoods (Lei et al., 2025).

When compared to the fundamental limits described in Sec. 4, we see that the PD models are lower bounded by $R(D/2, \infty)$, and the SD models are are lower bounded by the RDP function $R(D, 0)$ but outperform $R(D/2, \infty)$ when the rate is not too small. Although the fundamental RDP limits should be interpreted operationally with perception measured as Wasserstein and not sliced Wasserstein, we empirically verify that on Gaussians, sliced Wasserstein is faithful to Wasserstein in Appendix. E. The performance of $n = 1$ RCC (i.e., each dimension of $\boldsymbol{x}$ is compressed with RCC separately) and $n = 8$ RCC is shown in Fig. 7a. Performance improves with increasing dimension. However, the 8-dimensional RCC is outperformed by SD-LTC, and additionally has complexity exponential in dimension and rate; SD-LTC does not suffer the same high complexity. We show the RDP achieved by deterministic NTC in Fig. 7b; at low rates the lack of randomness prevents it from enforcing the perception constraint. At larger rates, its performance coincides with SD-NTC.

5.2 Real-World Sources

We use MNIST (Lecun et al., 1998), Physics and Speech datasets (Yang and Mandt, 2022). These contain grayscale images of dimension 28×28, physics measurements of dimension 16, and audio signals of dimension 33 respectively. We use a latent dimension of $n_L = 8$ for the first two and $n_L = 16$ for Speech. We use the integer lattice for NTC models; for MNIST/Physics, we use the E_8 lattice, and for Speech, we use the Λ_{16} lattice (Barnes and Wall, 1959). The corresponding RDP tradeoff is shown in Fig. 5. Due to lack of randomness, deterministic NTC and LTC are unable to enforce the perception constraint at lower rates, no matter how large λ_2 in (2) is set. Similar to the Gaussian case, performance improves with better lattices and increased shared randomness, demonstrating the benefits of lattices and shared randomness described in the prior sections translate to real-world sources that require nonlinear transforms. For QSD-LTC, we use self-similar nested lattices with a nesting ratios of 2 and 3, corresponding to $R_c = \log 2 = 1$ and $R_c = \log 3 \approx 1.58$

9

respectively. Performance increases with R_c (Fig. 6). A full comparison across all models/datasets is shown in Figs. 8, 9 and 10. Overall, SD-LTC achieves the RDP tradeoffs. For a fixed lattice, QSD-LTC, with $R_c = \log 3$, can nearly achieve the performance of SD-LTC, which uses $R_c = \infty$.

5.3 Ablation Study

We perform an ablation study on lattice choice and training of PD-LTC with STE or the noisy proxy. We use the D_n^* lattice for SD-LTC in Fig. 11 on Speech. Its performance lies between integer and Barnes-Wall lattices, which aligns with the fact that the D_n packing efficiency lies between those two lattices. This supports our result in Thm. 4.3 that performance is optimal when the lattices pack space more efficiently. For the noisy proxy, we use it to train PD-LTC, but this may result in a train/test mismatch, since unlike SD-LTC, the noisy proxy does not equal the rate under hard quantization. A comparison of the two in Fig. 12 shows there is not much difference in the resulting performance.

6 Conclusion and Limitations

We investigate low-complexity, high-performing compressors for the RDP tradeoff. We propose combining dithered LQ with neural compression, which supports different amounts of shared randomness. Under infinite and no shared randomness, we show SD-LTC and PD-LTC achieve optimality on the Gaussian source. We empirically verify that performance improves with increased shared randomness and improved lattice efficiency across synthetic and real-world data. Future work may address: (i) expanding the range of R_c in QSD-LTC, (ii) theoretical analysis of QSD-LTC, which may require new tools developed for dither vectors defined over nested lattices, and (iii) extension to SOTA image compression architectures, which would require careful integration of random dithering with hyperprior models that implicitly use a deterministic dither.

Disclaimer.   This paper was prepared by Eric Lei prior to his employment at JPMorgan Chase & Co.. Therefore, this paper is not a product of the Research Department of JPMorgan Chase & Co. or its affiliates. Neither JPMorgan Chase & Co. nor any of its affiliates makes any explicit or implied representation or warranty and none of them accept any liability in connection with this paper, including, without limitation, with respect to the completeness, accuracy, or reliability of the information contained herein and the potential legal, compliance, tax, or accounting effects thereof. This document is not intended as investment research or investment advice, or as a recommendation, offer, or solicitation for the purchase or sale of any security, financial instrument, financial product or service, or to be used in any way for evaluating the merits of participating in any transaction.

References

E. Agustsson and L. Theis. Universally quantized neural compression. *Advances in neural information processing systems*, 33:12367–12376, 2020.

E. Agustsson, M. Tschannen, F. Mentzer, R. Timofte, and L. V. Gool. Generative adversarial networks for extreme learned image compression. In *Proceedings of the IEEE/CVF International Conference on Computer Vision*, pages 221–231, 2019.

E. Agustsson, D. Minnen, G. Toderici, and F. Mentzer. Multi-realism image compression with a conditional generator. In *Proceedings of the IEEE/CVF Conference on Computer Vision and Pattern Recognition*, pages 22324–22333, 2023.

J. Ballé, P. A. Chou, D. Minnen, S. Singh, N. Johnston, E. Agustsson, S. J. Hwang, and G. Toderici. Nonlinear transform coding. *IEEE Journal of Selected Topics in Signal Processing*, 15(2):339–353, 2020.

J. Ballé, D. Minnen, S. Singh, S. J. Hwang, and N. Johnston. Variational image compression with a scale hyperprior. In *International Conference on Learning Representations*, 2018. URL https://openreview.net/forum?id=rkcQFMZRb.

W. Banaszczyk. New bounds in some transference theorems in the geometry of numbers. *Mathematische Annalen*, 296(4):625–635, 1993.

E. S. Barnes and G. E. Wall. Some extreme forms defined in terms of abelian groups. *Journal of the Australian Mathematical Society*, 1(1):47–63, 1959. doi: 10.1017/S1446788700025064.

Y. Blau and T. Michaeli. Rethinking lossy compression: The rate-distortion-perception tradeoff. In *International Conference on Machine Learning*, pages 675–685. PMLR, 2019.

N. Bonneel, J. Rabin, G. Peyré, and H. Pfister. Sliced and radon wasserstein barycenters of measures. *J. Math. Imaging Vis.*, 51(1):22–45, Jan. 2015. ISSN 0924-9907. doi: 10.1007/s10851-014-0506-3. URL https://doi.org/10.1007/s10851-014-0506-3.

J. Chen, L. Yu, J. Wang, W. Shi, Y. Ge, and W. Tong. On the rate-distortion-perception function. *IEEE Journal on Selected Areas in Information Theory*, 3(4):664–673, 2022.

J. H. Conway and N. J. A. Sloane. On the voronoi regions of certain lattices. *SIAM Journal on Algebraic Discrete Methods*, 5(3):294–305, 1984. doi: 10.1137/0605031. URL https://doi.org/10.1137/0605031.

J. H. Conway and N. J. A. Sloane. *Sphere Packings, Lattices, and Groups*. Grundlehren der mathematischen Wissenschaften. Springer, New York, NY, 1999. ISBN 978-0-387-98585-5.

P. Cuff. Distributed channel synthesis. *IEEE Transactions on Information Theory*, 59(11):7071–7096, 2013.

L. Dinh, J. Sohl-Dickstein, and S. Bengio. Density estimation using real NVP. In *International Conference on Learning Representations*, 2017. URL https://openreview.net/forum?id=HkpbnH9lx.

A. Gersho and R. M. Gray. *Vector quantization and signal compression*, volume 159. Springer Science & Business Media, 2012.

Y. Hamdi, A. B. Wagner, and D. Gündüz. The rate-distortion-perception trade-off: The role of private randomness. *arXiv preprint arXiv:2404.01111*, 2024a.

Y. Hamdi, A. B. Wagner, and D. Gunduz. The rate-distortion-perception trade-off with algorithmic realism. In *Workshop on Machine Learning and Compression, NeurIPS 2024*, 2024b. URL https://openreview.net/forum?id=fFkbEL1bMO.

D. He, Z. Yang, H. Yu, T. Xu, J. Luo, Y. Chen, C. Gao, X. Shi, H. Qin, and Y. Wang. Po-elic: Perception-oriented efficient learned image coding. In *Proceedings of the IEEE/CVF Conference on Computer Vision and Pattern Recognition*, pages 1764–1769, 2022.

S. Kudo, Y. Bandoh, S. Takamura, and M. Kitahara. LVQ-VAE:end-to-end hyperprior-based variational image compression with lattice vector quantization, 2023. URL https://openreview.net/forum?id=1pGmKJvneD7.

Y. Lecun, L. Bottou, Y. Bengio, and P. Haffner. Gradient-based learning applied to document recognition. *Proceedings of the IEEE*, 86(11):2278–2324, 1998. doi: 10.1109/5.726791.

E. Lei, H. Hassani, and S. Saeedi Bidokhti. Neural estimation of the rate-distortion function with applications to operational source coding. *IEEE Journal on Selected Areas in Information Theory*, 3(4):674–686, 2022. doi: 10.1109/JSAIT.2023.3273467.

E. Lei, H. Hassani, and S. S. Bidokhti. Approaching rate-distortion limits in neural compression with lattice transform coding. In *The Thirteenth International Conference on Learning Representations*, 2025. URL https://openreview.net/forum?id=Tv36j85SqR.

C. T. Li. Channel simulation: Theory and applications to lossy compression and differential privacy. *Found. Trends Commun. Inf. Theory*, 21(6):847–1106, Dec. 2024. ISSN 1567-2190. doi: 10.1561/0100000141. URL https://doi.org/10.1561/0100000141.

C. T. Li and A. El Gamal. Strong functional representation lemma and applications to coding theorems. *IEEE Transactions on Information Theory*, 64(11):6967–6978, 2018.

M. Li, J. Klejsa, and W. B. Kleijn. On distribution preserving quantization. *arXiv preprint arXiv:1108.3728*, 2011.

C. Ling and J.-C. Belfiore. Achieving awgn channel capacity with lattice gaussian coding. *IEEE Transactions on Information Theory*, 60(10):5918–5929, 2014. doi: 10.1109/TIT.2014.2332343.

C. Ling, L. Luzzi, J.-C. Belfiore, and D. Stehlé. Semantically secure lattice codes for the gaussian wiretap channel. *IEEE Transactions on Information Theory*, 60(10):6399–6416, 2014. doi: 10.1109/TIT.2014.2343226.

L. Liu, Y. Yan, C. Ling, and X. Wu. Construction of capacity-achieving lattice codes: Polar lattices. *IEEE Transactions on Communications*, 67(2):915–928, 2019. doi: 10.1109/TCOMM.2018. 2876113.

L. Liu, J. Shi, and C. Ling. Polar lattices for lossy compression. *IEEE Transactions on Information Theory*, 67(9):6140–6163, 2021. doi: 10.1109/TIT.2021.3097965.

L. Liu, S. Lyu, C. Ling, and B. Bai. On the quantization goodness of polar lattices. *arXiv preprint arXiv:2405.04051*, 2024.

H.-A. Loeliger. Averaging bounds for lattices and linear codes. *IEEE Transactions on Information Theory*, 43(6):1767–1773, 1997. doi: 10.1109/18.641543.

R. Matsumoto. Introducing the perception-distortion tradeoff into the rate-distortion theory of general information sources. *IEICE Communications Express*, 7(11):427–431, 2018.

F. Mentzer, G. D. Toderici, M. Tschannen, and E. Agustsson. High-fidelity generative image compression. *Advances in Neural Information Processing Systems*, 33, 2020.

D. Micciancio and O. Regev. Worst-case to average-case reductions based on gaussian measures. In *45th Annual IEEE Symposium on Foundations of Computer Science*, pages 372–381, 2004. doi: 10.1109/FOCS.2004.72.

M. J. Muckley, A. El-Nouby, K. Ullrich, H. Jégou, and J. Verbeek. Improving statistical fidelity for neural image compression with implicit local likelihood models. In *International Conference on Machine Learning*, pages 25426–25443. PMLR, 2023.

V. M. Panaretos and Y. Zemel. Statistical aspects of wasserstein distances. *Annual review of statistics and its application*, 6(1):405–431, 2019.

O. Regev. On lattices, learning with errors, random linear codes, and cryptography. *Journal of the ACM (JACM)*, 56(6):1–40, 2009.

N. Saldi, T. Linder, and S. Yüksel. Output constrained lossy source coding with limited common randomness. *IEEE Transactions on Information Theory*, 61(9):4984–4998, 2015. doi: 10.1109/ TIT.2015.2450721.

F. Santambrogio. Optimal transport for applied mathematicians. calculus of variations, pdes and modeling. 2015. URL https://www.math.u-psud.fr/~filippo/OTAM-cvgmt.pdf.

G. Serra, P. A. Stavrou, and M. Kountouris. Computation of rate-distortion-perception function under f-divergence perception constraints. In *2023 IEEE International Symposium on Information Theory (ISIT)*, pages 531–536. IEEE, 2023.

N. Stephens-Davidowitz. *On the Gaussian measure over lattices*. Phd thesis, New York University, 2017.

M. Talagrand. Transportation cost for gaussian and other product measures. *Geometric & Functional Analysis GAFA*, 6(3):587–600, 1996. doi: 10.1007/BF02249265. URL https://doi.org/10. 1007/BF02249265.

L. Theis and E. Agustsson. On the advantages of stochastic encoders. In *Neural Compression: From Information Theory to Applications – Workshop @ ICLR 2021*, 2021. URL https:// openreview.net/forum?id=FZ0f-znv62.

L. Theis and N. Y. Ahmed. Algorithms for the communication of samples. In K. Chaudhuri, S. Jegelka, L. Song, C. Szepesvari, G. Niu, and S. Sabato, editors, *Proceedings of the 39th International Conference on Machine Learning*, volume 162 of *Proceedings of Machine Learning Research*, pages 21308–21328. PMLR, 17–23 Jul 2022. URL https://proceedings.mlr.press/v162/theis22a.html.

L. Theis and A. B. Wagner. A coding theorem for the rate-distortion-perception function. In *Neural Compression: From Information Theory to Applications – Workshop @ ICLR 2021*, 2021. URL https://openreview.net/forum?id=BzUaLGtKecs.

L. Theis, T. Salimans, M. D. Hoffman, and F. Mentzer. Lossy compression with gaussian diffusion. *arXiv preprint arXiv:2206.08889*, 2022.

M. Tschannen, E. Agustsson, and M. Lucic. Deep generative models for distribution-preserving lossy compression. *Advances in neural information processing systems*, 31, 2018.

C. Villani. *Optimal Transport: Old and New*. Grundlehren der mathematischen Wissenschaften. Springer Berlin Heidelberg, 2016. ISBN 9783662501801. URL https://books.google.com/books?id=5p8SDAEACAAJ.

A. B. Wagner. The rate-distortion-perception tradeoff: The role of common randomness. *arXiv preprint arXiv:2202.04147*, 2022.

Z. Yan, F. Wen, R. Ying, C. Ma, and P. Liu. On perceptual lossy compression: The cost of perceptual reconstruction and an optimal training framework. In *International Conference on Machine Learning*, pages 11682–11692. PMLR, 2021.

R. Yang and S. Mandt. Lossy image compression with conditional diffusion models. *Advances in Neural Information Processing Systems*, 36, 2024.

Y. Yang and S. Mandt. Towards empirical sandwich bounds on the rate-distortion function. In *International Conference on Learning Representations*, 2022. URL https://openreview.net/forum?id=H4PmOqSZDY.

Y. Yang, S. Mandt, and L. Theis. An introduction to neural data compression. *Foundations and Trends® in Computer Graphics and Vision*, 15(2):113–200, 2023. ISSN 1572-2740. doi: 10.1561/0600000107. URL http://dx.doi.org/10.1561/0600000107.

Y. Yang, J. C. Will, and S. Mandt. Progressive compression with universally quantized diffusion models. *arXiv preprint arXiv:2412.10935*, 2024.

R. Zamir and M. Feder. On lattice quantization noise. *IEEE Transactions on Information Theory*, 42 (4):1152–1159, 1996. doi: 10.1109/18.508838.

R. Zamir, B. Nazer, Y. Kochman, and I. Bistritz. *Lattice Coding for Signals and Networks: A Structured Coding Approach to Quantization, Modulation and Multiuser Information Theory*. Cambridge University Press, 2014.

G. Zhang, J. Qian, J. Chen, and A. Khisti. Universal rate-distortion-perception representations for lossy compression. *Advances in Neural Information Processing Systems*, 34:11517–11529, 2021.

X. Zhang and X. Wu. Lvqac: Lattice vector quantization coupled with spatially adaptive companding for efficient learned image compression. In *Proceedings of the IEEE/CVF Conference on Computer Vision and Pattern Recognition*, pages 10239–10248, 2023.

W. Zhao and G. Qian. The second and fourth moments of discrete gaussian distributions over lattices. *Journal of Mathematics*, 2024(1):7777881, 2024. doi: https://doi.org/10.1155/2024/7777881. URL https://onlinelibrary.wiley.com/doi/abs/10.1155/2024/7777881.

R. Zhou and C. Tian. Staggered quantizers for perfect perceptual quality: A connection between quantizers with common randomness and without. In *First 'Learn to Compress' Workshop @ ISIT 2024*, 2024. URL https://openreview.net/forum?id=keX3SC5cOt.

J. Ziv. On universal quantization. *IEEE Transactions on Information Theory*, 31(3):344–347, 1985. doi: 10.1109/TIT.1985.1057034.

A Reverse Channel Coding

A.1 RCC Preliminaries

Reverse channel coding (RCC), also known as channel simulation, devises schemes for sending a sample from a prescribed distribution with a rate constraint (Cuff, 2013; Li, 2024), and typically assumes shared randomness. Since RDP requires randomized reconstructions, RCC can be applied to RDP, and in fact is a technique used to prove RDP coding theorems; Theis and Wagner (2021) use the one-shot RCC scheme of Li and El Gamal (2018), and Saldi et al. (2015); Wagner (2022) use channel synthesis results of Cuff (2013). We focus our discussion here on the particular RCC scheme of Li and El Gamal (2018), defined below.

Definition A.1 (One-shot reverse channel coding (RCC) via the Poisson functional representation (Li and El Gamal, 2018))**.** Let $X \sim P_X$ be the source, and $P_{\hat{X}|X}$ be a channel we wish to simulate. Define $Q_{\hat{X}}$ to be the $\hat{X}$-marginal of the joint distribution $P_X P_{\hat{X}|X}$. Suppose that the same sequence of $\tau_1, \tau_2, \cdots \sim \mathrm{Exp}(1)$ and $\hat{X}_1, \hat{X}_1, \ldots \overset{\text{i.i.d.}}{\sim} Q_{\hat{X}}$ are generated at both the encoder and decoder (requiring infinite shared randomness U). Let $W_i = \sum_{j=1}^{i} \tau_j$. Given a source realization $X = x$, the encoder computes

$$K = \arg \min_i W_i \frac{dQ_{\hat{X}}}{dP_{\hat{X}|X}(\cdot|x)}(\hat{X}_i), \tag{17}$$

and entropy-codes it. The decoder simply outputs $\hat{X}_K$. By Li and El Gamal (2018), it holds that $\hat{X}_K|\{X = x\} \sim P_{\hat{X}|X}(\cdot|x)$. Additionally, the rate satisfies

$$H(K|U) \leq I(X; \hat{X}) + \log(I(X; \hat{X}) + 1) + 4. \tag{18}$$

Remark A.2. The one-shot RCC technique above enables immediate achievability results for informational quantities, such as the rate-distortion-perception function $R(D, P)$, by simulating the channel $P_{\hat{X}|X}$ that achieves the infimum in (1). Due to the fact that the reconstruction $\hat{X}_K$ has distribution equal to the channel $P_{\hat{X}|X}$, any constraint in the informational quantity, such as the expected distortion constraint, or the perception constraint, is automatically satisfied by RCC. The $I(X; \hat{X})$ term in (18) then becomes equal to the informational quantity $R(D, P)$. Applying this scheme to i.i.d. blocks yields the asymptotic result. This is the approach used to prove achievability in Theis and Wagner (2021).

A.2 RCC as Randomized VQ

The scheme in Def. A.1 essentially chooses a random codebook at both the encoder and decoder. The encoder chooses a codeword $\hat{X}_K$ according to the criterion in (17), which may appear abstract at first glance. However, the following two propositions show that when the channel $P_{\hat{X}|X}$ used to simulate is chosen to be RD- or RDP-achieving, it becomes clear that (17) uses a minimum-distance codebook search similar to VQ.

Proposition A.3 (RCC on the rate-distortion-achieving channel; Prop. 1 of Lei et al. (2022))**.** *Let* $P_{\hat{X}|X}$ *be the rate-distortion-achieving channel, i.e., the channel achieving the infimum of* $R(D, \infty)$. *Then the density ratio satisfies*

$$\frac{dP_{\hat{X}|X}(\cdot|x)}{dQ_{\hat{X}}}(\hat{x}) = \frac{e^{-\beta \Delta(x,\hat{x})}}{\mathbb{E}_{\hat{X}' \sim Q_{\hat{X}}}[e^{-\beta \Delta(x,\hat{X}')}]}, \tag{19}$$

and (17) *is equivalent to*

$$K = \arg \min_i \Delta(x, \hat{X}_i) + \frac{1}{\beta} \ln W_i, \tag{20}$$

where $\beta > 0$ *is the unique Lagrange multiplier determining* $I(X; \hat{X}) = R(D, \infty)$ *at* $D = \mathbb{E}_{P_X P_{\hat{X}|X}}[\Delta(X, \hat{X})]$.

Proposition A.4 (RCC on the RDP-achieving channel with f-divergence perception). *Assume that the perception is measured by $\delta(P_X, P_{\hat{X}}) = D_f(P_X \| P_{\hat{X}})$, a f-divergence. Let $P_{\hat{X}|X}$ be the RDP-achieving channel that achieves* (1). *Serra et al. (2023) show that the density ratio satisfies*

$$\frac{dP_{\hat{X}|X}(\cdot|x)}{dQ_{\hat{X}}}(\hat{x}) = \frac{e^{-\beta_1 \Delta(x,\hat{x}) - \beta_2 g(P_X, Q_{\hat{X}}, \hat{x})}}{\mathbb{E}_{\hat{X}' \sim Q_{\hat{X}}}\left[e^{-\beta_1 \Delta(x,\hat{X}') - \beta_2 g(P_X, Q_{\hat{X}}, \hat{X}')}\right]}, \tag{21}$$

where $g(P_X, Q_{\hat{X}}, \hat{x}') := f\left(\frac{dP_X}{dQ_{\hat{X}}}(\hat{x})\right) - \frac{dP_X}{dQ_{\hat{X}}}(\hat{x})\partial f\left(\frac{dP_X}{dQ_{\hat{X}}}(\hat{x})\right)$, and $\beta_1, \beta_2 > 0$ are the unique Lagrange multipliers determining $I(X; \hat{X}) = R(D, P)$, at $D = \mathbb{E}_{P_X P_{\hat{X}|X}}[\Delta(X, \hat{X})]$ and $P = D_f(P_X \| P_{\hat{X}})$. Therefore, (17) *is equivalent to*

$$K = \arg\min_i \Delta(x, \hat{X}_i) + \frac{\beta_2}{\beta_1} g(P_X, Q_{\hat{X}}, \hat{X}_i) + \frac{1}{\beta_1} \ln W_i. \tag{22}$$

Proof. The proof follows Lei et al. (2022, Prop. 1), using (21) instead of (19). □

Remark A.5. The above two propositions imply that RCC with the RD- or RDP-achieving channels result the encoder searching for the random codeword in $\{\hat{X}_1, \hat{X}_2, \dots\}$ that is closest to the source realization x in terms of the distortion metric Δ, regularized by $\ln W_i$, which enforces the rate constraint; for the RDP case, it is additionally regularized by $g(P_X, Q_{\hat{X}}, \hat{X}_i')$ which enforces the perception constraint.

Thus, when taking distortion into account, RCC can be seen as a sort of randomized VQ that finds the minimum-distance codeword (which are random). Despite its optimality for RDP, RCC is of high complexity (exponential in rate and dimension), and requires infinite shared randomness.

Remark A.6. A closed-form for the density ratio of the RDP-achieving channel $P_{\hat{X}|X}$ for when the perception is measured by squared 2-Wasserstein (which is the focus of our paper) is currently not known. However, we conjecture that similar to (19) and (21), it will consist of a $e^{-\beta' \Delta(x,\hat{x})}$ term in the numerator, which will result in (17) having $\Delta(x, \hat{X}_i)$ in the objective. Another slight discrepancy to our setup is that the n-letter operational perception in Serra et al. (2023) for the f-divergence perception RDP function is measured in the weak-sense (see Sec. 2). We are focused on the strong-sense setting as it more faithfully describes practical usage.

A.3 RCC Implementation Details

To simulate RCC, one can implement the scheme in Def. A.1 and use (20) or (22) for finding the index to entropy-code. For the Gaussian source, the RDP-achieving channel and output marginal is given in Remark 4.2; we can directly implement (17) in closed-form since these distributions are Gaussian. This is what is done for the results in Fig. 7a. Since it is not possible to generate an infinite number of samples $\hat{X}_i$, we generate a codebook $N = 10,000$ samples instead. Following Li and El Gamal (2018), the index K is entropy-coded using a Zipf distribution with parameter $\lambda = 1 + 1/(I(X; \hat{X} + e^{-1}\log e + 1)$. A full algorithm describing the encoding and decoding process can be found in Theis and Ahmed (2022) as well as Lei et al. (2022).

B Additional Experimental Details

For the synthetic (i.i.d. Gaussian source), we set $n_L = 8$, g_a and g_s to be linear functions, as the constructions in Thm. 4.3 and Thm. 4.5 suggest this to be sufficient for optimality, and use the $\mathbb{Z}_8$ and E_8 lattices. To cover the RDP tradeoff, we sweep a variety of λ_1, λ_2 values. For the Speech and Physics datasets, we use MLPs for g_a and g_s of depth 3, hidden dimension 100, and softplus nonlinearities. For MNIST, we follow the same exact experimental setup of Blau and Michaeli (2019), including model architecture, and using the test Wasserstein distance via the discriminator neural network. For NTC models, we use the factorized p_y of Ballé et al. (2018), and for LTC models, we use the RealNVP normalizing flow (Dinh et al., 2017). All models are trained for 100 epochs on the

training data split, and reported metrics are averaged over the test split. Training is performed on a NVIDIA RTX5000 GPU.

For the real-world sources, we swept λ_1 (the distortion weight) and kept λ_2 (the perception weight) fixed to a positive value. This allows us to compare rate-distortion and rate-perception tradeoffs across methods; note that the two plots should be examined jointly together, and that the individual plots do not show the rate-perception (or rate-distortion) performance for a fixed distortion (or perception).

C Additional Empirical Results

Figures pertaining to the experimental evaluation in Sec. 5, such as ablation studies, are shown here.

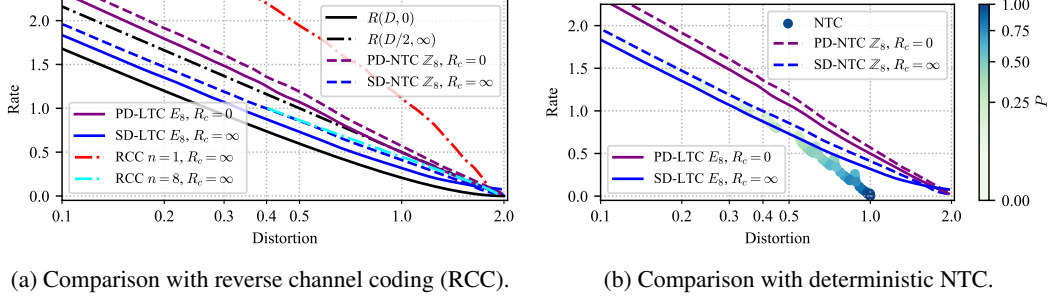(a) Comparison with reverse channel coding (RCC).   (b) Comparison with deterministic NTC.

Figure 7: Gaussian RDP results, comparing PD-LTC and SD-LTC with RCC and deterministic NTC.

Figure 8: RDP tradeoff of all models on MNIST. QSD-NTC/LTC-Γ corresponds to QSD-NTC/LTC with a nesting ratio of Γ.

Figure 9: RDP tradeoff of all models on Physics. QSD-NTC/LTC-Γ corresponds to QSD-NTC/LTC with a nesting ratio of Γ.

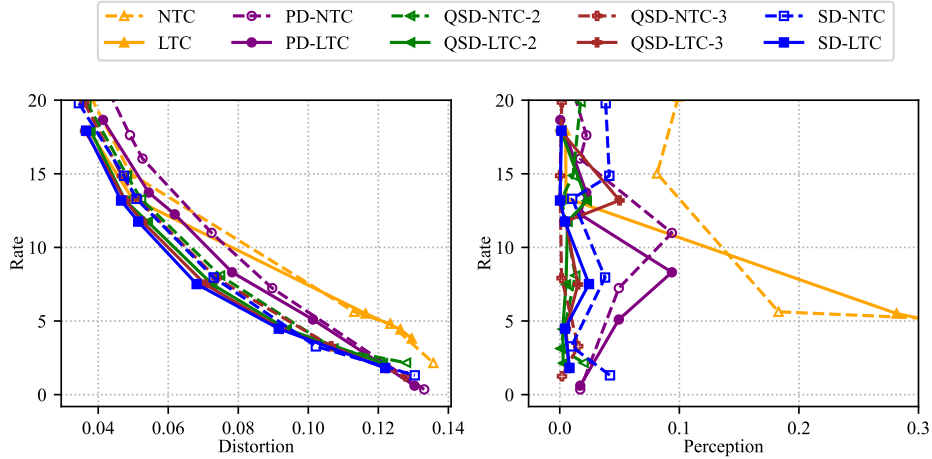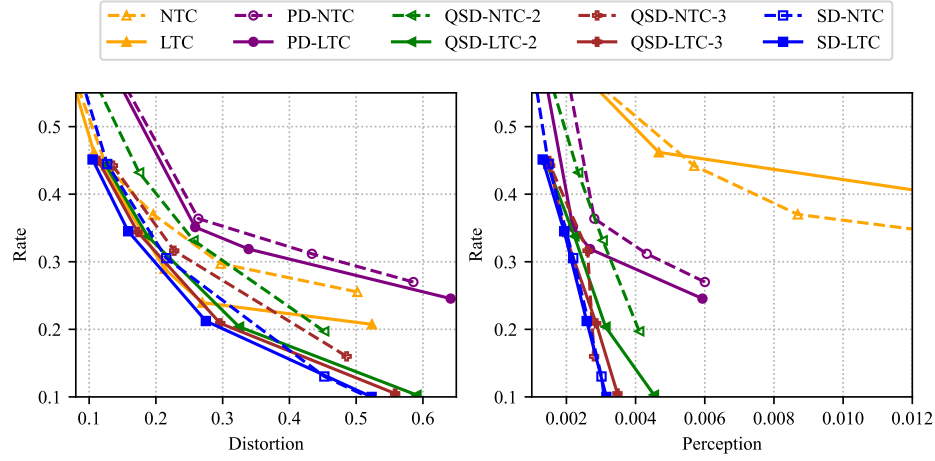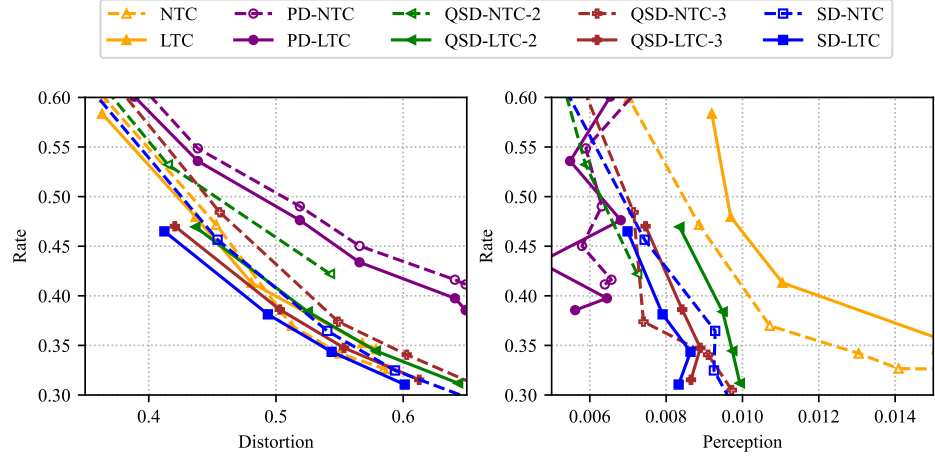Figure 10: RDP tradeoff of all models on Speech. QSD-NTC/LTC-Γ corresponds to QSD-NTC/LTC with a nesting ratio of Γ.
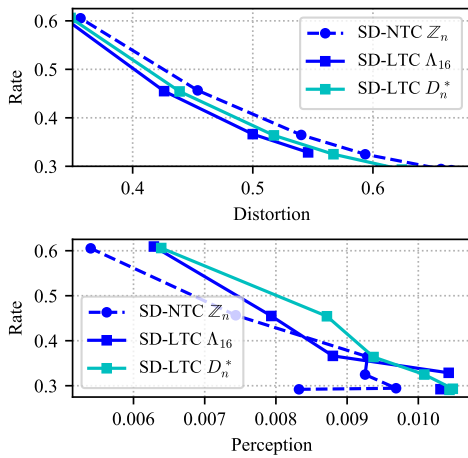

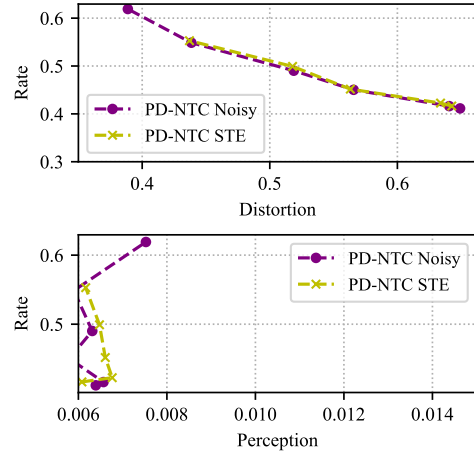Figure 11: Comparing different lattice choices for SD-LTC, on Speech.

Figure 12: Comparing straight-through estimator (STE) with hard quantization vs. noisy proxy for PD-NTC, on Speech.

D   Proofs

D.1   Proof of Proposition 3.3

Proof. By the crypto lemma (Zamir et al., 2014), we have that $\hat{\boldsymbol{x}}_{\mathsf{SD}} = Q_\Lambda(\boldsymbol{x} - \boldsymbol{u}) + \boldsymbol{u} \stackrel{d}{=} \boldsymbol{x} + \boldsymbol{u}$. Then

$$\frac{1}{n}\,\mathbb{E}\big[\|\boldsymbol{x} - \hat{\boldsymbol{x}}_{\mathsf{SD}}\|^2\big] = \frac{1}{n}\,\mathbb{E}[\|\boldsymbol{u}\|^2] = \sigma^2(\Lambda), \tag{23}$$

the second moment of the lattice. Additionally,

$$\frac{1}{n}\,\mathbb{E}\big[\|\boldsymbol{x} - \hat{\boldsymbol{x}}_{\mathsf{PD}}\|^2\big] = \frac{1}{n}\,\mathbb{E}\big[\|\boldsymbol{x} - Q_\Lambda(\boldsymbol{x}) - s\boldsymbol{u}\|^2\big] \tag{24}$$

$$= \frac{1}{n}\,\mathbb{E}\big[\|\boldsymbol{x} - Q_\Lambda(\boldsymbol{x})\|^2\big] + \frac{1}{n}s^2\,\mathbb{E}[\|\boldsymbol{u}\|^2] \tag{25}$$

$$= s^2\sigma^2(\Lambda) + \frac{1}{n}\,\mathbb{E}\big[\|\boldsymbol{x} - Q_\Lambda(\boldsymbol{x})\|^2\big] \tag{26}$$

$$\geq s^2\sigma^2(\Lambda) \tag{27}$$

$$\geq \sigma^2(\Lambda), \tag{28}$$

as desired. $\qquad\square$

D.2   Proof of Theorem 4.3

Theorem D.1 (Optimality of SD-LTC for Gaussian sources (Thm. 4.3 in main text)). *Let* $X_1, X_2, \dots \stackrel{\text{i.i.d.}}{\sim} \mathcal{N}(0, \sigma^2)$. *For any* P *and* D *satisfying* $0 \leq P \leq \sigma^2$ *and* $0 < D \leq 2\sigma^2$, *there exists a sequence of SD-LTCs* $\{(g_a^{(n)}, g_s^{(n)}, \Lambda^{(n)})\}_{n=1}^\infty$ *such that the achieved rate, distortion, and perception satisfy*

$$\lim_{n\to\infty} \frac{1}{n} H(Q_{\Lambda^{(n)}}(g_a^{(n)}(X^n) - \boldsymbol{u})|\boldsymbol{u}) = R(D, P), \tag{29}$$

$$\lim_{n\to\infty} \frac{1}{n} \mathbb{E}\Big[\|X^n - \hat{X}^n\|_2^2\Big] \leq D, \tag{30}$$

$$\lim_{n\to\infty} \frac{1}{n} W_2^2(X^n, \hat{X}^n) \leq P, \tag{31}$$

where $\hat{X}^n = g_s^{(n)}(Q_{\Lambda^{(n)}}(g_a^{(n)}(X^n) - \boldsymbol{u}) + \boldsymbol{u})$, *and* $\boldsymbol{u} \sim \text{Unif}(\mathcal{V}_0(\Lambda^{(n)}))$.

Proof. We first focus on the case when $\sqrt{P} < \sigma - \sqrt{|\sigma^2 - D|}$. Define the sequence of DLTCs $\{(g_a^{(n)}, g_s^{(n)}, \Lambda^{(n)})\}_{n=1}^\infty$ as follows. Choose $\Lambda^{(n)}$ to be a sequence of sphere-bound-achieving lattices, i.e., $\lim_{n\to\infty} G(\Lambda^{(n)}) = \frac{1}{2\pi e}$, where $G(\cdot)$ is the normalized second moment, such that the second moment $\sigma^2(\Lambda^{(n)}) = \eta^2 := \sigma^2 \left[\frac{\sigma^2(\sigma - \sqrt{P})^2}{\frac{1}{4}(\sigma^2 + (\sigma - \sqrt{P})^2 - D)^2} - 1 \right]$. Set $g_a^{(n)}(\boldsymbol{v}) = \boldsymbol{v}$ to be identity mapping, and set $g_s^{(n)}(\boldsymbol{v}) = \frac{\sigma - \sqrt{P}}{\sqrt{\sigma^2 + \eta^2}}\boldsymbol{v}$.

We first verify the perception constraint is satisfied. Fix $\epsilon > 0$. From Zamir et al. (2014, Thm. 7.3.3), we have that

$$\frac{1}{n} D_{\mathsf{KL}}(\boldsymbol{u}^{(n)}\|\boldsymbol{z}) < \frac{\epsilon^2}{2\sigma^2} \tag{32}$$

for n sufficiently large, where $\boldsymbol{u}^{(n)} \sim \text{Unif}(\mathcal{V}_0(\Lambda^{(n)}))$ is uniform over the fundamental cell of $\Lambda^{(n)}$, and $\boldsymbol{z} \sim \mathcal{N}(0, \eta^2 I_n)$. Let $P_{\tilde{Y}^n} = \mathcal{N}\left(0, (\sigma - \sqrt{P})^2 I_n\right)$. Then, for n sufficiently large,

$$\frac{1}{n}D_{\mathsf{KL}}(P_{\hat{X}^n}||P_{\tilde{Y}^n}) = \frac{1}{n}D_{\mathsf{KL}}\left(\frac{\sigma - \sqrt{P}}{\sqrt{\sigma^2 + \eta^2}}(X^n + \boldsymbol{u}^{(n)})||\frac{\sigma - \sqrt{P}}{\sqrt{\sigma^2 + \eta^2}}(X^n + \boldsymbol{z})\right) \quad (33)$$

$$= \frac{1}{n}D_{\mathsf{KL}}(X^n + \boldsymbol{u}^{(n)}||X^n + \boldsymbol{z}) \quad (34)$$

$$\leq \frac{1}{n}D_{\mathsf{KL}}(\boldsymbol{u}^{(n)}||\boldsymbol{z}) \quad (35)$$

$$\leq \frac{\epsilon^2}{2\sigma^2}, \quad (36)$$

where (33) holds by the crypto lemma (Zamir et al., 2014, Ch. 4.1), (34) holds since KL-divergence is invariant to affine transformations, and (35) is by data-processing inequality. Thus, for n sufficiently large,

$$\frac{1}{\sqrt{n}}W_2\left(P_{X^n}, P_{\hat{X}^n}\right) \leq \frac{1}{\sqrt{n}}W_2(P_{X^n}, P_{\tilde{Y}^n}) + \frac{1}{\sqrt{n}}W_2\left(P_{\hat{X}^n}, P_{\tilde{Y}^n}\right) \quad (37)$$

$$\leq \frac{1}{\sqrt{n}}W_2(P_{X^n}, P_{\tilde{Y}^n}) + \frac{1}{\sqrt{n}} \cdot \sqrt{2\sigma^2 \cdot D_{\mathsf{KL}}\left(P_{\hat{X}^n}||P_{\tilde{Y}^n}\right)} \quad (38)$$

$$\leq \frac{1}{\sqrt{n}}W_2(P_{X^n}, P_{\tilde{Y}^n}) + \epsilon \quad (39)$$

$$\leq \frac{1}{\sqrt{n}}\sqrt{\sum_{i=1}^{n}W_2^2\left(P_{X_i}, \mathcal{N}\left(0, (\sigma - \sqrt{P})^2\right)\right)} + \epsilon \quad (40)$$

$$= W_2\left(\mathcal{N}(0, \sigma^2), \mathcal{N}\left(0, (\sigma - \sqrt{P})^2\right)\right) + \epsilon \quad (41)$$

$$= \sqrt{P} + \epsilon, \quad (42)$$

where (37) holds since Wasserstein distance satisfies triangle inequality, (38) is by Talagrand (1996), and (40) holds by properties of 2-Wasserstein distance on product measures (Panaretos and Zemel, 2019). By continuity of $z \mapsto z^2$, we have $\lim_{n\to\infty}\frac{1}{n}W_2^2(X^n, \hat{X}^n) \leq P$.

The rate achieved will satisfy

$$\lim_{n\to\infty}\frac{1}{n}H(Q_{\Lambda^{(n)}}(X^n - \boldsymbol{u}^{(n)})|\boldsymbol{u}^{(n)}) = \lim_{n\to\infty}\frac{1}{n}I(X^n; X^n + \boldsymbol{u}^{(n)}) \quad (43)$$

$$= I(X; X + Z) \quad (44)$$

$$= \frac{1}{2}\log\left(1 + \frac{\sigma^2}{\eta^2}\right) \quad (45)$$

$$= \frac{1}{2}\log\left(1 + \frac{1}{\frac{\sigma^2(\sigma-\sqrt{P})^2}{\frac{1}{4}\left(\sigma^2+(\sigma-\sqrt{P})^2-D\right)^2} - 1}\right) \quad (46)$$

$$= \frac{1}{2}\log\frac{\sigma^2(\sigma - \sqrt{P})^2}{\sigma^2(\sigma - \sqrt{P})^2 - \frac{1}{4}\left(\sigma^2 + (\sigma - \sqrt{P})^2 - D\right)^2}, \quad (47)$$

where $\boldsymbol{u}^{(n)}$ is uniform over $\Lambda^{(n)}$, and $Z \sim \mathcal{N}(0, \eta^2)$. Here, (43) holds by Zamir et al. (2014, Thm. 5.2.1), and (44) is due to Zamir and Feder (1996, Thm. 3).

The distortion satisfies

$$\lim_{n\to\infty} \frac{1}{n} \mathbb{E}\left[\left\|X^n - \hat{X}^n\right\|^2\right] = \lim_{n\to\infty} \frac{1}{n} \mathbb{E}\left[\left\|X^n - \frac{\sigma - \sqrt{P}}{\sqrt{\sigma^2 + \eta^2}}(X^n + \boldsymbol{u}^{(n)})\right\|_2^2\right] \tag{48}$$

$$= \lim_{n\to\infty} \frac{1}{n} \mathbb{E}\left[\left\|X^n - \frac{\sigma - \sqrt{P}}{\sqrt{\sigma^2 + \eta^2}}(X^n + Z^n)\right\|_2^2\right], \tag{49}$$

where $Z^n \sim \mathcal{N}(0, \eta^2 I)$. Here, (48) holds by crypto lemma, and (49) holds since X^n and $\boldsymbol{u}^{(n)}$ are independent, so the squared norm becomes a sum of second moments of X^n and $\boldsymbol{u}^{(n)}$, and $\mathbb{E}[\|\boldsymbol{u}^{(n)}\|^2] = \mathbb{E}[\|Z^n\|^2]$. Since X^n and Z^n are now i.i.d.,

$$\lim_{n\to\infty} \frac{1}{n} \mathbb{E}\left[\left\|X^n - \hat{X}^n\right\|^2\right] = \mathbb{E}\left[\left(X - \frac{\sigma - \sqrt{P}}{\sqrt{\sigma^2 + \eta^2}}(X + Z)\right)^2\right] \tag{50}$$

$$= \left(1 - \frac{\sigma - \sqrt{P}}{\sqrt{\sigma^2 + \eta^2}}\right)^2 \sigma^2 + \left(\frac{(\sigma - \sqrt{P})^2}{\sigma^2 + \eta^2}\right) \eta^2 \tag{51}$$

$$= \sigma^2 + (\sigma - \sqrt{P})^2 - 2\sigma^2 \frac{\sigma - \sqrt{P}}{\sqrt{\sigma^2 + \eta^2}} \tag{52}$$

$$= \sigma^2 + (\sigma - \sqrt{P})^2 - (\sigma^2 + (\sigma - \sqrt{P})^2 - D) \tag{53}$$

$$= D. \tag{54}$$

For the case when $\sqrt{P} \geq \sigma - \sqrt{|\sigma^2 - D|}$, we use a sequence of DLTCs with $g_a^{(n)}(\boldsymbol{v}) = \boldsymbol{v}$, $g_s^{(n)}(\boldsymbol{v}) = \left(\frac{\sigma^2 - D}{\sigma^2}\right)\boldsymbol{v}$, and a sequence of sphere-bound-achieving lattices $\Lambda^{(n)}$ with second moment $\sigma^2(\Lambda) = \frac{1}{1/D - 1/\sigma^2}$. For the perception constraint, by following the proof of the perception constraint in the previous case, except with $P_{\tilde{Y}^n} = \mathcal{N}(0, (\sigma^2 - D)I_n)$ and $\boldsymbol{z} \sim \mathcal{N}\left(0, \frac{1}{(1/D - 1/\sigma^2)}I_n\right)$, we have that

$$\frac{1}{\sqrt{n}} W_2\left(P_{X^n}, P_{\hat{X}^n}\right) \leq W_2\left(\mathcal{N}(0, \sigma^2), \mathcal{N}(0, \sigma^2 - D)\right) + \epsilon \tag{55}$$

$$= \sigma - \sqrt{|\sigma^2 - D|} + \epsilon \tag{56}$$

$$\leq \sqrt{P} + \epsilon, \tag{57}$$

for any $\epsilon > 0$ and n sufficiently large, where the last step is by the assumption that $\sqrt{P} \geq \sigma - \sqrt{|\sigma^2 - D|}$. The result follows again by continuity of $z \mapsto z^2$. For the rate and distortion constraints of

$$\lim_{n\to\infty} \frac{1}{n} H(Q_{\Lambda^{(n)}}(X^n - \boldsymbol{u}^{(n)})|\boldsymbol{u}^{(n)}) = \max\left\{\frac{1}{2}\log\frac{\sigma^2}{D}, 0\right\}, \tag{58}$$

and

$$\lim_{n\to\infty} \frac{1}{n} \mathbb{E}\left[\left\|X^n - \hat{X}^n\right\|^2\right] = D, \tag{59}$$

the proof follows that of Zamir et al. (2014, Thm. 5.6.1).

$\square$

D.3 Proof of Theorem 4.5

We now consider the case when the encoder and decoder do not have access to infinite shared randomness. Unlike Thm. 4.3, Thm. 4.5 cannot make use of the additive channel equivalence, and we instead rely on results from lattice Gaussian coding (Ling and Belfiore, 2014). We first introduce several important concepts of lattice Gaussians, then establish several lemmas that will be used to prove Thm. 4.5.

Definition D.2 (Lattice Gaussian Distribution). A lattice Gaussian random variable $\boldsymbol{y} \sim \mathcal{N}_\Lambda(\boldsymbol{c}, \sigma^2)$ supported on a (shifted) lattice $\Lambda + \boldsymbol{c} \subseteq \mathbb{R}^n$ has PMF

$$q_{\boldsymbol{y}}(\boldsymbol{\lambda}) = \frac{\rho_\sigma(\boldsymbol{\lambda})}{\rho_\sigma(\Lambda + \boldsymbol{c})}, \quad \boldsymbol{\lambda} \in \Lambda + \boldsymbol{c}, \tag{60}$$

where $\rho_\sigma(\boldsymbol{y}) = e^{-\frac{1}{2\sigma^2}\|\boldsymbol{y}\|^2}$ and $\rho_\sigma(\Lambda) = \sum_{\boldsymbol{\lambda} \in \Lambda} \rho_\sigma(\boldsymbol{\lambda})$.

For a more in-depth introduction, see Stephens-Davidowitz (2017). The proof of Thm. 4.5 relies on known results regarding the lattice Gaussian second moment and entropy; see Ling and Belfiore (2014); Regev (2009); Banaszczyk (1993) for details.

Two tools which will be used throughout the proof are the (i) flatness factor of a lattice, and (ii) a vanishing error probability of maximum a posteriori (MAP) decoding of a lattice Gaussian signal sent over an AWGN channel. For (i), the flatness factor (Ling et al., 2014) of a lattice Λ is defined as

$$\epsilon_\Lambda(\gamma) := \max_{\boldsymbol{x} \in \mathcal{V}_0(\Lambda)} |V(\Lambda)\rho_{\gamma,\Lambda}(\boldsymbol{x}) - 1|, \tag{61}$$

where $\rho_{\gamma,\Lambda}(\boldsymbol{x}) = \frac{1}{(2\pi\gamma^2)^{n/2}} \sum_{\boldsymbol{\lambda} \in \Lambda} e^{-\frac{\|\boldsymbol{x}-\boldsymbol{\lambda}\|^2}{2\gamma^2}}$. For (ii), suppose we wish to send $\boldsymbol{y} \sim \mathcal{N}_\Lambda(\boldsymbol{c}, \sigma^2 - \nu)$ over an AWGN channel with noise $\boldsymbol{z} \sim \mathcal{N}(0, \nu I_n)$. Ling and Belfiore (2014) show that given the received signal $\tilde{\boldsymbol{x}} = \boldsymbol{y} + \boldsymbol{z}$, the MAP decoder of $\boldsymbol{y}$ given $\tilde{\boldsymbol{x}}$ is given by $Q_{\Lambda-\boldsymbol{c}}(\alpha\tilde{\boldsymbol{x}})$, where $\alpha = \frac{\sigma^2 - \nu}{\sigma^2}$.

The high-level approach in the proof of Thm. 4.5 is to analyze the rate, distortion, and perception when compressing $\tilde{\boldsymbol{x}} = \boldsymbol{y} + \boldsymbol{z}$, following Liu et al. (2021; 2024). This is because $P_{\tilde{\boldsymbol{x}}}$ approximates $\mathcal{N}(0, \sigma^2 I_n)$, with the approximation error given by the flatness factor $\epsilon_\Lambda\left(\sqrt{\frac{(\sigma^2-\nu)\nu}{\sigma^2}}\right)$ (Ling and Belfiore, 2014; Regev, 2009). With a vanishing MAP error probability, $Q_\Lambda(\alpha\tilde{\boldsymbol{x}}) \approx \boldsymbol{y}$, and the overall system can be statistically analyzed using the properties of $\boldsymbol{y}$, which is a lattice Gaussian. We refer the reader to Ling et al. (2014); Ling and Belfiore (2014); Liu et al. (2021) for further details of lattice Gaussian coding.

The next result describes the scaling of the lattice covering radius $r_{\mathrm{cov}}(\Lambda) := \min\{r : \Lambda + \mathcal{B}(\mathbf{0}, r)$ is a covering of $\mathbb{R}^n\}$, where $\Lambda + \mathcal{B}(\mathbf{0}, r)$ is the set composed of spheres of radius r centered at all lattice vectors of Λ (Zamir et al., 2014). This allows one to bound the ℓ^2 error between a vector and its lattice-quantized version by $O(n^{1/2})$.

Lemma D.3. *Let Λ be a n-dimensional lattice with volume $C_1^{n/2}$. Then its covering radius satisfies*

$$r_{\mathrm{cov}}(\Lambda) \le C_2 \sqrt{\frac{\pi e}{2}} \left(\frac{C_1}{\pi}\right)^{1/2} \left[\left(\frac{n}{2}\right)!\right]^{1/n} = O(n^{1/2}), \tag{62}$$

for a positive constant C_2.

Proof. Using results in Zamir et al. (2014, Ch. 3),

$$r_{\mathrm{cov}}(\Lambda) = \rho_{\mathrm{cov}}(\Lambda) \cdot r_{\mathrm{eff}}(\Lambda) \tag{63}$$

$$\le C\sqrt{\frac{\pi e}{2}} \left[\frac{V(\Lambda)}{V_n}\right]^{1/n} \tag{64}$$

$$= C\sqrt{\frac{\pi e}{2}} \left[\frac{C_1^{n/2}}{\frac{\pi^{n/2}}{(n/2)!}}\right]^{1/n} \tag{65}$$

$$= C\sqrt{\frac{\pi e}{2}} \left(\frac{C_1}{\pi}\right)^{1/2} [(n/2)!]^{1/n} \tag{66}$$

$$= O(n^{1/2}), \tag{67}$$

where C is a constant, ρ_{cov} is the covering efficiency, r_{eff} is the effective lattice radius, and V_n is the volume of a n-dimensional unit ball, following Zamir et al. (2014, Ch. 3). $\square$

The next lemma bounds the second moment of $Q(\alpha\tilde{\boldsymbol{x}})$, which is used to bound the error terms.

Lemma D.4. *Let $\tilde{x} = y + z$, $y \sim \mathcal{N}_\Lambda(c, \sigma^2 - \nu)$ and $z \sim \mathcal{N}(0, \nu I_n)$. Let $\alpha = \frac{\sigma^2 - \nu}{\sigma^2}$. If $\{\Lambda^{(n)}\}_{n=1}^\infty$ is a sequence of lattices that is AWGN-good with vanishing error probability of MAP decoding of y given $\tilde{x}$, then for any $\epsilon > 0$,*

$$\mathbb{E}[\|Q(\alpha\tilde{x})\|^2] \leq \mathbb{E}[\|y\|^2] + \epsilon, \tag{68}$$

for sufficiently large n.

Proof. The second moment of $Q(\alpha\tilde{x})$ satisfies

$$\mathbb{E}\big[\|Q(\alpha\tilde{x})\|^2\big] = \mathbb{E}\Big[\|Q(\alpha\tilde{x})\|^2 \mathbb{1}\{\mathcal{E}^{\complement}\}\Big] + \mathbb{E}\big[\|Q(\alpha\tilde{x})\|^2 \mathbb{1}\{\mathcal{E}\}\big] \tag{69}$$

$$= \mathbb{E}\Big[\|y\|^2 \mathbb{1}\{\mathcal{E}^{\complement}\}\Big] + \mathbb{E}\big[\|Q(\alpha\tilde{x})\|^2 \mathbb{1}\{\mathcal{E}\}\big] \tag{70}$$

$$\leq \mathbb{E}\big[\|y\|^2\big] \|\mathbb{1}\{\mathcal{E}^{\complement}\}\|_\infty + \mathbb{E}\big[\|Q(\alpha\tilde{x})\|^2 \mathbb{1}\{\mathcal{E}\}\big] \tag{71}$$

$$= \mathbb{E}\big[\|y\|^2\big] + \mathbb{E}\big[\|Q(\alpha\tilde{x})\|^2 \mathbb{1}\{\mathcal{E}\}\big] \tag{72}$$

$$\leq \mathbb{E}\big[\|y\|^2\big] + \sqrt{\mathbb{E}[\|Q(\alpha\tilde{x})\|^4]\, \mathbb{P}(\mathcal{E})}, \tag{73}$$

where in (71) we use Hölder's inequality, and the last step is by Cauchy-Schwarz. The second term involving the error event vanishes as follows. We have that

$$\|Q(\alpha\tilde{x})\|^4 \leq 8\|Q(\alpha\tilde{x}) - \alpha\tilde{x}\|^4 + 8\|\alpha\tilde{x}\|^4 \tag{74}$$

$$\leq 8\|y - \alpha\tilde{x}\|^4 + 8\|\alpha\tilde{x}\|^4 \tag{75}$$

$$= 8\|(1 - \alpha)y - \alpha z\|^4 + 8\|\alpha y + \alpha z\|^4, \tag{76}$$

where (74) is by triangle inequality and Cauchy-Schwarz, and (75) holds since Q finds the closest vector to $\alpha\tilde{x}$. We have that the expectations satisfy

$$\mathbb{E}\big[\|(1 - \alpha)y - \alpha z\|^4\big] \tag{77}$$

$$\leq (1 - \alpha)^4\, \mathbb{E}[\|y\|^4] + \alpha^4\, \mathbb{E}[\|z\|^4] + \alpha^2(1 - \alpha)^2\, \mathbb{E}[\langle y, z\rangle^2] + 2(1 - \alpha)^2 \alpha^2\, \mathbb{E}[\|y\|^2 \|z\|^2] \tag{78}$$

$$\leq 3(1 - \alpha)^4(\sigma^2 - \nu)^2 n + \alpha^4 \nu^2 n(n + 2) + 3\alpha^2(1 - \alpha)^2\, \mathbb{E}[\|y\|^2]\, \mathbb{E}[\|z\|^2] \tag{79}$$

$$\leq 3(1 - \alpha)^4(\sigma^2 - \nu)^2 n + \alpha^4 \nu^2 n(n + 2) + 3\alpha^2(1 - \alpha)^2(\sigma^2 - \nu)\nu n^2 \tag{80}$$

$$= O(n^2), \tag{81}$$

and

$$\mathbb{E}\big[\|\alpha y + \alpha z\|^4\big] = \alpha^4\, \mathbb{E}\big[\|y\|^4\big] + \alpha^4\, \mathbb{E}\big[\|z\|^4\big] + \alpha^4\, \mathbb{E}[\langle y, z\rangle^2] + 2\alpha^4\, \mathbb{E}\big[\|y\|^2 \|z\|^2\big] \tag{82}$$

$$\leq 3\alpha^4(\sigma^2 - \nu)^2 n + \alpha^4 \nu^2 n(n + 2) + 3\alpha^4\, \mathbb{E}\big[\|y\|^2 \|z\|^2\big] \tag{83}$$

$$= 3\alpha^4(\sigma^2 - \nu)^2 n + \alpha^4 \nu^2 n(n + 2) + 3\alpha^4(\sigma^2 - \nu)\nu n^2 \tag{84}$$

$$= O(n^2), \tag{85}$$

for n sufficiently large. This implies that

$$\mathbb{E}\big[\|Q(\alpha\tilde{x})\|^4\big] \leq 8\, \mathbb{E}\big[\|(1 - \alpha)y - \alpha z\|^4\big] + 8\, \mathbb{E}\big[\|\alpha y + \alpha z\|^4\big] = O(n^2), \tag{86}$$

and therefore

$$\frac{1}{n}\sqrt{\mathbb{E}[\|Q(\alpha\tilde{x})\|^4]\, \mathbb{P}(\mathcal{E})} < \epsilon \tag{87}$$

for n sufficiently large since $\lim_{n\to\infty} \mathbb{P}(\mathcal{E}) = 0$. $\qquad\square$

Before proving Thm. 4.5, we first prove a lemma which describes an achievable RDP region of pre/post-scaled lattice quantization with private dithering on the Gaussian source that makes the relationship between the flatness factors and the scaling s explicit. Ensuring that all flatness factors vanish would imply a single-letter characterization of the achievable RDP region for the near-perfect perception regime, which is what Thm. 4.5 provides.

Lemma D.5. *Let $X_1, X_2, \ldots \overset{\text{i.i.d.}}{\sim} \mathcal{N}(0, \sigma^2)$. Let $\nu \in (0, \sigma^2)$, $\alpha = \frac{\sigma^2 - \nu}{\sigma^2}$, and $s > 0$, $\beta > 0$ be constants satisfying*

$$(\sigma^2 - \nu) + s^2 \frac{(\sigma^2 - \nu)\nu}{\sigma^2} = \frac{\sigma^2}{\beta^2}. \tag{88}$$

Let $\tilde{\boldsymbol{x}} = \boldsymbol{y} + \boldsymbol{z}$, $\boldsymbol{y} \sim \mathcal{N}_\Lambda(\boldsymbol{c}, \sigma^2 - \nu)$ and $\boldsymbol{z} \sim \mathcal{N}(0, \nu I_n)$. If $\{\Lambda^{(n)}\}_{n=1}^\infty$ is a sequence of lattices that is AWGN-good with vanishing error probability of MAP decoding of $\boldsymbol{y}$ given $\tilde{\boldsymbol{x}}$, and is also quantization-good, then for any $\epsilon > 0$,

$$\frac{1}{n} H(Q_{\Lambda^{(n)}}(\alpha X^n)) \le \frac{1}{1 - 4\epsilon_z} \left(\frac{1}{2} \log \frac{\sigma^2}{\nu} + \epsilon_h + \epsilon \right), \tag{89}$$

$$\frac{1}{n} \mathbb{E}[\|X^n - \hat{X}^n\|^2] \le \frac{1}{1 - 4\epsilon_z} \left((1 - \beta)^2 (\sigma^2 - \nu) + \nu + s^2 \beta^2 \frac{(\sigma^2 - \nu)\nu}{\sigma^2} + \epsilon \right), \tag{90}$$

$$\frac{1}{\sqrt{n}} W_2(P_{X^n}, P_{\hat{X}^n}) \le \sqrt{8\sigma^2 \epsilon_u} + \beta \sqrt{8\epsilon_z \left(2\frac{\sigma^2 - \nu}{1 - 4\epsilon_z} + 2s^2 \frac{(\sigma^2 - \nu)\nu}{\sigma^2} \right)} + \epsilon, \tag{91}$$

for n sufficiently large, where $\hat{X}^n = \beta(Q_{\Lambda^{(n)}}(\alpha X^n) + s\boldsymbol{u})$, $\boldsymbol{u} \sim \text{Unif}(\mathcal{V}(\Lambda^{(n)}))$. In the above, $\epsilon_h = -\frac{\log(1 - \epsilon_1)}{n} + \frac{\pi(t^{-4} + 1)\epsilon_1}{n(1 - \epsilon_1)}$, and

$$\epsilon_1 := \epsilon_{\Lambda^{(n)}} \left(\frac{\sqrt{\sigma^2 - \nu}}{\sqrt{\frac{\pi}{\pi - t}}} \right), \quad \epsilon_z := \epsilon_{\Lambda^{(n)}} \left(\sqrt{\frac{(\sigma^2 - \nu)\nu}{\sigma^2}} \right), \quad \epsilon_u := \epsilon_{\Lambda^{(n)}} \left(\sqrt{\frac{(\sigma^2 - \nu)\nu s^2}{\sigma^2 + s^2 \nu}} \right)$$

$$\tag{92}$$

are flatness factors of lattices $\Lambda^{(n)}$, with $0 < t < 1/e$.

Proof. Since the lattice sequence is AWGN-good, choose the fundamental volume to satisfy $V(\Lambda^{(n)}) = \left(2\pi e \frac{(\sigma^2 - \nu)\nu}{\sigma^2} (1 + \epsilon_2) \right)^{\frac{n}{2}}$, where $\epsilon_2 \xrightarrow{n \to \infty} 0$, following that of Ling and Belfiore (2014). In the following, we denote the quantizers $Q_{\Lambda^{(n)}}$ as Q with the dependence on the lattice implicit.

Define $\mathcal{E} := \{Q(\alpha\tilde{\boldsymbol{x}}) \ne \boldsymbol{y}\}$ as the "error" event of MAP decoding of $\boldsymbol{y}$ given $\tilde{\boldsymbol{x}}$ (Ling and Belfiore, 2014, Lemma 11). By assumption, $\lim_{n \to \infty} \mathbb{P}(\mathcal{E}) = 0$. Finally, since the lattices are sphere-bound-achieving, we have that the lattice NSM satisfies $\lim_{n \to \infty} G(\Lambda^{(n)}) \to \frac{1}{2\pi e}$. The vanishing error probability and sphere-bound-achieving properties of the lattices will be used to establish the convergence.

We first address the perception constraint. By triangle inequality,

$$\frac{1}{\sqrt{n}} W_2(P_{X^n}, P_{\hat{X}^n}) \le \frac{1}{\sqrt{n}} W_2(P_{X^n}, P_{\beta(Q(\alpha\tilde{\boldsymbol{x}}) + s\boldsymbol{u})}) + \frac{1}{\sqrt{n}} W_2(P_{\hat{X}^n}, P_{\beta(Q(\alpha\tilde{\boldsymbol{x}}) + s\boldsymbol{u})}). \tag{93}$$

We first bound the second term on the right. By Regev (2009, Claim 3.9) and Ling and Belfiore (2014, Lemma 9), $|dP_{\tilde{\boldsymbol{x}}}(\boldsymbol{x}) - dP_{X^n}(\boldsymbol{x})| \le 4\epsilon_z dP_{X^n}(\boldsymbol{x}), \forall \boldsymbol{x}$. By the change of variable formula, this implies $|dP_{\alpha\tilde{\boldsymbol{x}}}(\boldsymbol{x}) - dP_{\alpha X^n}(\boldsymbol{x})| \le 4\epsilon_z dP_{\alpha X^n}(\boldsymbol{x})$. Additionally, we have that for any $\boldsymbol{\lambda} \in \Lambda$,

$$\Pr(Q(\alpha\tilde{\boldsymbol{x}}) = \boldsymbol{\lambda}) = \int_{\mathcal{V}_0 + \boldsymbol{\lambda}} dP_{\alpha\tilde{\boldsymbol{x}}} \le \int_{\mathcal{V}_0 + \boldsymbol{\lambda}} (1 + 4\epsilon_z) dP_{\alpha X^n} = (1 + 4\epsilon_z) \Pr(Q(\alpha X^n) = \boldsymbol{\lambda}), \tag{94}$$

and $\Pr(Q(\alpha\tilde{\boldsymbol{x}}) = \boldsymbol{\lambda}) \ge (1 - 4\epsilon_z) \Pr(Q(\alpha X^n) = \boldsymbol{\lambda})$ follows similarly. Thus

$$|\Pr(Q(\alpha\tilde{\boldsymbol{x}}) = \boldsymbol{\lambda}) - \Pr(Q(\alpha X^n) = \boldsymbol{\lambda})| \le 4\epsilon_z \Pr(Q(\alpha X^n) = \boldsymbol{\lambda}). \tag{95}$$

Finally, we have

$$dP_{Q(\alpha\tilde{\boldsymbol{x}}) + s\boldsymbol{u}}(\boldsymbol{w}) = \sum_{\boldsymbol{\lambda} \in \Lambda} \Pr(Q(\alpha\tilde{\boldsymbol{x}}) = \boldsymbol{\lambda}) dP_{s\boldsymbol{u}}(\boldsymbol{w} - \boldsymbol{\lambda}) \tag{96}$$

$$\le \sum_{\boldsymbol{\lambda} \in \Lambda} (1 + 4\epsilon_z) \Pr(Q(\alpha X^n) = \boldsymbol{\lambda}) dP_{s\boldsymbol{u}}(\boldsymbol{w} - \boldsymbol{\lambda}) \tag{97}$$

$$= (1 + 4\epsilon_z) dP_{Q(\alpha X^n) + s\boldsymbol{u}}(\boldsymbol{w}), \tag{98}$$

where the other direction follows similarly. Thus

$$|dP_{Q(\alpha\tilde{\boldsymbol{x}}) + s\boldsymbol{u}}(\boldsymbol{w}) - dP_{Q(\alpha X^n) + s\boldsymbol{u}}(\boldsymbol{w})| \le 4\epsilon_z dP_{Q(\alpha X^n) + s\boldsymbol{u}}(\boldsymbol{w}). \tag{99}$$

for any $\boldsymbol{w}$. This implies

$$\frac{1}{\beta\sqrt{n}}W_2\big(P_{\hat{X}^n}, P_{\beta(Q(\alpha\tilde{\boldsymbol{x}})+s\boldsymbol{u})}\big) = \frac{1}{\sqrt{n}}W_2\big(P_{Q(\alpha X^n)+s\boldsymbol{u}}, P_{Q(\alpha\tilde{\boldsymbol{x}}+s\boldsymbol{u})}\big) \tag{100}$$

$$\leq \frac{1}{\sqrt{n}}\sqrt{2\int \|\boldsymbol{w}\|^2 |dP_{Q(\alpha\tilde{\boldsymbol{x}})+s\boldsymbol{u}}(\boldsymbol{w}) - dP_{Q(\alpha X^n)+s\boldsymbol{u}}(\boldsymbol{w})|d\boldsymbol{w}} \tag{101}$$

$$\leq \sqrt{8\epsilon_z \frac{1}{n}\mathbb{E}[\|Q(\alpha X^n) + s\boldsymbol{u}\|^2]}, \tag{102}$$

where (101) is by Villani (2016, Thm. 6.15). To bound the second norm, we first get

$$\frac{1}{n}\mathbb{E}[\|Q(\alpha X^n) + s\boldsymbol{u}\|^2] \leq 2\frac{1}{n}\mathbb{E}[\|Q(\alpha X^n)\|^2] + 2\frac{1}{n}\mathbb{E}[\|s\boldsymbol{u}\|^2] \tag{103}$$

$$= 2\frac{1}{n}\mathbb{E}[\|Q(\alpha X^n)\|^2] + 2s^2\frac{(\sigma^2 - \nu)\nu}{\sigma^2}. \tag{104}$$

The second moment of $Q(\alpha X^n)$ satisfies

$$\mathbb{E}[\|Q(\alpha X^n)\|^2] = \sum_{\boldsymbol{\lambda}} \|\boldsymbol{\lambda}\|^2 \Pr(Q(\alpha X^n) = \boldsymbol{\lambda}) \tag{105}$$

$$= \sum_{\boldsymbol{\lambda}} \|\boldsymbol{\lambda}\|^2 (\Pr(Q(\alpha\tilde{\boldsymbol{x}}) = \boldsymbol{\lambda}) - \Pr(Q(\alpha X^n) = \boldsymbol{\lambda})) + \sum_{\boldsymbol{\lambda}} \|\boldsymbol{\lambda}\|^2 \Pr Q(\alpha\tilde{\boldsymbol{x}}) = \boldsymbol{\lambda}) \tag{106}$$

$$\leq 4\epsilon_z \mathbb{E}[\|Q(\alpha X^n)\|^2] + \mathbb{E}[\|Q(\alpha\tilde{\boldsymbol{x}})\|^2], \tag{107}$$

where the last step is by (95). Thus for n sufficiently large,

$$\frac{1}{n}\mathbb{E}[\|Q(\alpha X^n)\|^2] \leq \frac{1}{1-4\epsilon_z}\frac{1}{n}\mathbb{E}[\|Q(\alpha\tilde{\boldsymbol{x}})\|^2] \tag{108}$$

$$\leq \frac{1}{1-4\epsilon_z}(\sigma^2 - \nu), \tag{109}$$

where the last step is by Lemma D.4 and Banaszczyk (1993). Combining with (102) and (104),

$$\frac{1}{\sqrt{n}}W_2\big(P_{\hat{X}^n}, P_{\beta(Q(\alpha\tilde{\boldsymbol{x}})+s\boldsymbol{u})}\big) \leq \beta\sqrt{8\epsilon_z\left(2\frac{\sigma^2 - \nu}{1-4\epsilon_z} + 2s^2\frac{(\sigma^2 - \nu)\nu}{\sigma^2}\right)}. \tag{110}$$

For the first term on the right of (93), we again apply triangle inequality:

$$\frac{1}{\sqrt{n}}W_2(P_{X^n}, P_{\beta(Q(\alpha\tilde{\boldsymbol{x}})+s\boldsymbol{u})}) \leq \underbrace{\frac{1}{\sqrt{n}}W_2(P_{X^n}, P_{\beta(\boldsymbol{y}+s\boldsymbol{u})})}_{A} + \underbrace{\frac{1}{\sqrt{n}}W_2(P_{\beta(Q(\alpha\tilde{\boldsymbol{x}})+s\boldsymbol{u})}, P_{\beta(\boldsymbol{y}+s\boldsymbol{u})})}_{B}. \tag{111}$$

For term A, let $\tilde{\boldsymbol{z}} \sim \mathcal{N}\big(0, \frac{(\sigma^2-\nu)\nu}{\sigma^2}I_n\big)$ and $\boldsymbol{r} \sim \mathcal{N}\big(0, \frac{\sigma^2}{\beta^2}I_n\big)$. Then

$$\frac{1}{\sqrt{n}}W_2(P_{\boldsymbol{r}}, P_{\boldsymbol{y}+s\tilde{\boldsymbol{z}}}) \leq \frac{1}{\sqrt{n}}\sqrt{2\int \|\boldsymbol{w}\|^2 |dP_{\boldsymbol{r}} - dP_{\boldsymbol{y}+s\tilde{\boldsymbol{z}}}|d\boldsymbol{w}} \tag{112}$$

$$\leq \frac{1}{\sqrt{n}}\sqrt{8\epsilon_u \mathbb{E}_{\boldsymbol{r}}[\|\boldsymbol{r}\|^2]} \tag{113}$$

$$= \sqrt{8\epsilon_u\frac{\sigma^2}{\beta^2}}, \tag{114}$$

24

where (112) is by Villani (2016, Thm. 6.15), and (113) holds since s, β satisfy (88) and by applying Ling and Belfiore (2014, Lemma 9). Therefore

$$\frac{1}{\beta\sqrt{n}} W_2(P_{X^n}, P_{\beta(\boldsymbol{y}+s\boldsymbol{u})}) = \frac{1}{\sqrt{n}} W_2(P_{\boldsymbol{r}}, P_{\boldsymbol{y}+s\boldsymbol{u}}) \tag{115}$$

$$\leq \frac{1}{\sqrt{n}} W_2(P_{\boldsymbol{r}}, P_{\boldsymbol{y}+s\tilde{\boldsymbol{z}}}) + \frac{1}{\sqrt{n}} W_2(P_{\boldsymbol{y}+s\tilde{\boldsymbol{z}}}, P_{\boldsymbol{y}+s\boldsymbol{u}}) \tag{116}$$

$$\leq \sqrt{8\epsilon_u \frac{\sigma^2}{\beta^2}} + s \frac{1}{\sqrt{n}} W_2(P_{\boldsymbol{u}}, P_{\tilde{\boldsymbol{z}}}) \tag{117}$$

$$\leq \sqrt{8\epsilon_u \frac{\sigma^2}{\beta^2}} + s \frac{1}{\sqrt{n}} \sqrt{2 \frac{(\sigma^2 - \nu)\nu}{\sigma^2} D_{\mathsf{KL}}(\boldsymbol{u}||\tilde{\boldsymbol{z}})} \tag{118}$$

$$\leq \sqrt{8\epsilon_u \frac{\sigma^2}{\beta^2}} + \frac{\epsilon}{2\beta}, \tag{119}$$

where (117) holds by Ling and Belfiore (2014, Lemma 9) for n sufficiently large, and data processing inequality for W_2 (Santambrogio, 2015, Lemma 5.2), (118) holds by Talagrand (1996), and (119) holds because

$$\frac{1}{n} D_{\mathsf{KL}}(\boldsymbol{u}||\tilde{\boldsymbol{z}}) = \frac{1}{n} \mathbb{E}_{\boldsymbol{u}}[-\log p_{\tilde{\boldsymbol{z}}}(\boldsymbol{u})] - \frac{1}{n} H(\boldsymbol{u}) \tag{120}$$

$$= \frac{1}{n} \left[\frac{1}{2\ln 2 \frac{(\sigma^2-\nu)\nu}{\sigma^2}} \mathbb{E}_{\boldsymbol{u}}[\|\boldsymbol{u}\|^2] + \frac{n}{2} \log\left(2\pi \frac{(\sigma^2-\nu)\nu}{\sigma^2}\right) \right] - \frac{1}{n} \log V(\Lambda^{(n)}) \tag{121}$$

$$= G(\Lambda^{(n)}) \cdot 2\pi e \frac{1+\epsilon_2}{2\ln 2} + \frac{1}{2} \log \frac{1}{e(1+\epsilon_2)} \tag{122}$$

$$= \frac{1}{2\ln 2} \Big(G(\Lambda^{(n)}) \cdot 2\pi e(1+\epsilon_2) - 1 \Big) - \frac{1}{2} \log(1+\epsilon_2) \tag{123}$$

$$\overset{n\to\infty}{\longrightarrow} 0, \tag{124}$$

where we use the fact that $\frac{1}{n} \mathbb{E}[\|\boldsymbol{u}\|^2] = G(\Lambda^{(n)}) \cdot 2\pi e \cdot \frac{(\sigma^2-\nu)\nu}{\sigma^2}(1+\epsilon_2)$ and the lattice sequence is sphere-bound-achieving. Thus

$$A = \frac{1}{\sqrt{n}} W_2(P_{X^n}, P_{\beta(\boldsymbol{y}+\boldsymbol{u})}) \leq \sqrt{8\sigma^2\epsilon_u} + \frac{\epsilon}{2}. \tag{125}$$

For term B, let us first divide by β and analyze the squared 2-Wasserstein; this gives us $\frac{1}{n} W_2^2(P_{Q(\alpha\tilde{\boldsymbol{x}})+s\boldsymbol{u}}, P_{\boldsymbol{y}+s\boldsymbol{u}}) \leq \frac{1}{n} W_2^2(P_{Q(\alpha\tilde{\boldsymbol{x}})}, P_{\boldsymbol{y}})$ by Santambrogio (2015, Lemma 5.2). Let π be the coupling between $P_{Q(\alpha\tilde{\boldsymbol{x}})}, P_{\boldsymbol{y}}$ induced by the joint $P_{\tilde{\boldsymbol{x}},\boldsymbol{y}}$; i.e., $\hat{\boldsymbol{y}}, \boldsymbol{y} \sim \pi$ means that $\hat{\boldsymbol{y}} = Q(\alpha(\boldsymbol{y}+\boldsymbol{z}))$ with $\boldsymbol{z} \sim \mathcal{N}(0, \nu I_n)$ as defined above. Then,

$$\frac{1}{n} W_2^2(P_{Q(\alpha\tilde{\boldsymbol{x}})}, P_{\boldsymbol{y}}) = \frac{1}{n} \min_{\pi' \in \Pi(P_{Q(\alpha\tilde{\boldsymbol{x}})}, P_{\boldsymbol{y}})} \mathbb{E}_{\hat{\boldsymbol{y}}, \boldsymbol{y} \sim \pi'} \left[\|\hat{\boldsymbol{y}} - \boldsymbol{y}\|^2 \right] \tag{126}$$

$$\leq \frac{1}{n} \mathbb{E}_{\hat{\boldsymbol{y}}, \boldsymbol{y} \sim \pi} \left[\|\hat{\boldsymbol{y}} - \boldsymbol{y}\|^2 \right] = \frac{1}{n} \mathbb{E}_{\boldsymbol{y}, \boldsymbol{z}} \left[\|\hat{\boldsymbol{y}} - \boldsymbol{y}\|^2 \right] \tag{127}$$

$$= \frac{1}{n} \mathbb{E}_{\boldsymbol{y}, \boldsymbol{z}} \left[\|\hat{\boldsymbol{y}} - \boldsymbol{y}\|^2 \Big| \mathcal{E}^{\complement} \right] \mathbb{P}(\mathcal{E}^{\complement}) + \frac{1}{n} \mathbb{E}_{\boldsymbol{y}, \boldsymbol{z}} \left[\|\hat{\boldsymbol{y}} - \boldsymbol{y}\|^2 \mathbb{1}\{\mathcal{E}\} \right] \tag{128}$$

$$= \frac{1}{n} \mathbb{E}_{\boldsymbol{y}, \boldsymbol{z}} \left[\|\hat{\boldsymbol{y}} - \boldsymbol{y}\|^2 \mathbb{1}\{\mathcal{E}\} \right] \tag{129}$$

$$\leq \frac{1}{n} \sqrt{\mathbb{E}[\|\hat{\boldsymbol{y}} - \boldsymbol{y}\|^4] \mathbb{P}(\mathcal{E})} \tag{130}$$

where $\mathcal{E} := \{Q(\alpha\tilde{\boldsymbol{x}}) \neq \boldsymbol{y}\} = \{(\alpha-1)\boldsymbol{y} + \alpha\boldsymbol{z} \notin \mathcal{V}_0(\Lambda)\}$ is the "error" event that quantizing $\alpha\tilde{\boldsymbol{x}}$ does not equal the lattice Gaussian $\boldsymbol{y}$, and the last step is by Cauchy-Schwarz. For (129), we have

that $\mathbb{E}_{\boldsymbol{y},\boldsymbol{z}}\left[\|\hat{\boldsymbol{y}} - \boldsymbol{y}\|^2 \big| \mathcal{E}^{\complement}\right] = \mathbb{E}_{\boldsymbol{y},\boldsymbol{z}}\left[\|\hat{\boldsymbol{y}} - \boldsymbol{y}\|^2 | \hat{\boldsymbol{y}} = \boldsymbol{y}\right] = 0$. Note that

$$\|\hat{\boldsymbol{y}} - \boldsymbol{y}\| = \|\hat{\boldsymbol{y}} - \alpha\tilde{\boldsymbol{x}} + \alpha\tilde{\boldsymbol{x}} - \boldsymbol{y}\| \leq \|\hat{\boldsymbol{y}} - \alpha\tilde{\boldsymbol{x}}\| + \|\boldsymbol{y} - \alpha\tilde{\boldsymbol{x}}\| = \min_{\boldsymbol{y}' \in \Lambda^{(n)}} \|\boldsymbol{y}' - \alpha\tilde{\boldsymbol{x}}\| + \|\boldsymbol{y} - \alpha\tilde{\boldsymbol{x}}\|$$
(131)

$$\leq \|\boldsymbol{y} - \alpha\tilde{\boldsymbol{x}}\| + \|\boldsymbol{y} - \alpha\tilde{\boldsymbol{x}}\| = 2 \cdot \|\boldsymbol{y} - \alpha\tilde{\boldsymbol{x}}\|.$$
(132)

This implies that

$$\mathbb{E}\left[\|\hat{\boldsymbol{y}} - \boldsymbol{y}\|^4\right] \tag{133}$$

$$\leq 16\,\mathbb{E}\left[\|\boldsymbol{y} - \alpha\tilde{\boldsymbol{x}}\|^4\right] \tag{134}$$

$$= 16\,\mathbb{E}\left[\|(1-\alpha)\boldsymbol{y} - \alpha\boldsymbol{z}\|^4\right] \tag{135}$$

$$= 16(1-\alpha)^4\,\mathbb{E}[\|\boldsymbol{y}\|^4] + 16\alpha^4\,\mathbb{E}[\|\boldsymbol{z}\|^4] + 64P\alpha^2(1-\alpha)^2\,\mathbb{E}[\langle\boldsymbol{y},\boldsymbol{z}\rangle^2] + 32(1-\alpha)^2\alpha^2\,\mathbb{E}[\|\boldsymbol{y}\|^2\|\boldsymbol{z}\|^2]$$
(136)

where we use the fact that y, z are independent. Note that $\frac{1}{n}\mathbb{E}[\|\boldsymbol{y}\|^4] \leq 3(\sigma^2 - \nu)^2$ for n sufficiently large (Zhao and Qian, 2024; Micciancio and Regev, 2004), $\mathbb{E}[\|\boldsymbol{z}\|^4] = \nu^2 n(n+2)$, and $\mathbb{E}[\langle\boldsymbol{y},\boldsymbol{z}\rangle^2] \leq \mathbb{E}[\|\boldsymbol{y}\|^2\|\boldsymbol{z}\|^2] \leq \mathbb{E}[\|\boldsymbol{y}\|^2]\,\mathbb{E}[\|\boldsymbol{z}\|^2]$ by Cauchy-Schwarz and independence. Additionally, $\mathbb{E}[\|\boldsymbol{y}\|^2] \leq n(\sigma^2 - \nu)$ by Banaszczyk (1993). Therefore

$$\mathbb{E}\left[\|\hat{\boldsymbol{y}} - \boldsymbol{y}\|^4\right] \leq 48(1-\alpha)^4 \cdot (\sigma^2 - \nu)^2 n + 16\alpha^4 \cdot \nu^2 n(n+2) + 96\alpha^2(1-\alpha)^2\,\mathbb{E}[\|\boldsymbol{y}\|^2]\,\mathbb{E}[\|\boldsymbol{z}\|^2]$$
(137)

$$\leq 48(1-\alpha)^4 \cdot (\sigma^2 - \nu)^2 n + 16\alpha^4 \cdot \nu^2 n(n+2) + 96\alpha^2(1-\alpha)^2 n^2(\sigma^2 - \nu)\nu$$
(138)

$$= O(n^2). \tag{139}$$

By the choice of α, $Q(\alpha\tilde{\boldsymbol{x}})$ computes the MAP estimate of $\boldsymbol{y}$ (Ling and Belfiore, 2014, Prop. 3). Therefore,

$$\frac{1}{n}\sqrt{\mathbb{E}_{\boldsymbol{y},\boldsymbol{z}}[\|\hat{\boldsymbol{y}} - \boldsymbol{y}\|^4]\,\mathbb{P}(\mathcal{E})} \leq \frac{\epsilon^2}{4\beta^2}, \tag{140}$$

for n sufficiently large, since the error of the MAP estimate satisfies $\lim_{n\to\infty}\mathbb{P}(\mathcal{E}) = 0$. Hence

$$\frac{1}{\sqrt{n}}W_2(P_{\beta(Q(\alpha\tilde{\boldsymbol{x}})+s\boldsymbol{u})}, P_{\beta(\boldsymbol{y}+s\boldsymbol{u})}) \leq \frac{\beta}{\sqrt{n}}W_2(P_{Q(\alpha\tilde{\boldsymbol{x}})}, P_{\boldsymbol{y}}) \tag{141}$$

$$\overset{(129)}{\leq} \beta\sqrt{\frac{1}{n}\mathbb{E}_{\boldsymbol{y},\boldsymbol{z}}[\|\hat{\boldsymbol{y}} - \boldsymbol{y}\|^2\mathbb{1}\{\mathcal{E}\}]} \tag{142}$$

$$\overset{(140)}{\leq} \beta\frac{\epsilon}{2\beta} = \frac{\epsilon}{2}. \tag{143}$$

In conclusion, we have shown

$$\frac{1}{\sqrt{n}}W_2(P_{X^n}, P_{\hat{X}^n}) \leq \sqrt{8\sigma^2\epsilon_u} + \beta\sqrt{8\epsilon_z\left(2\frac{\sigma^2 - \nu}{1 - 4\epsilon_z} + 2s^2\frac{(\sigma^2 - \nu)\nu}{\sigma^2}\right)} + \epsilon. \tag{144}$$

Next, we address the distortion term. We have that

$$\frac{1}{n}\mathbb{E}_{X^n,\boldsymbol{u}}\left[\|X^n - \beta(Q(\alpha X^n) - s\boldsymbol{u})\|^2\right] = \mathbb{E}_{\boldsymbol{u}}\left[\underbrace{\frac{1}{n}\int\|\boldsymbol{x} - \beta(Q(\alpha\boldsymbol{x}) - s\boldsymbol{u})\|^2(dP_{X^n}(\boldsymbol{x}) - dP_{\tilde{\boldsymbol{x}}}(\boldsymbol{x}))d\boldsymbol{x}}_{S_1}\right]$$

$$+ \underbrace{\frac{1}{n}\mathbb{E}_{\tilde{\boldsymbol{x}},\boldsymbol{u}}\left[\|\tilde{\boldsymbol{x}} - \beta(Q(\alpha\tilde{\boldsymbol{x}}) - s\boldsymbol{u})\|^2\right]}_{S_2}. \tag{145}$$

26

By Regev (2009, Claim 3.9) and Ling and Belfiore (2014, Lemma 9), $|dP_{\tilde{\boldsymbol{x}}}(\boldsymbol{x}) - dP_{X^n}(\boldsymbol{x})| \leq 4\epsilon_z dP_{X^n}(\boldsymbol{x}), \forall \boldsymbol{x}$. The first term S_1 can be written as

$$S_1 \leq 4\epsilon_z \frac{1}{n} \int \|\boldsymbol{x} - \beta(Q(\alpha\boldsymbol{x}) - s\boldsymbol{u}')\|^2 dP_{X^n} = 4\epsilon_z \frac{1}{n} \mathbb{E}_{X^n}\big[\|X^n - \beta(Q(\alpha X^n) - s\boldsymbol{u}')\|^2\big], \tag{146}$$

for any $\boldsymbol{u}'$ and therefore

$$\frac{1}{n} \mathbb{E}_{X^n, \boldsymbol{u}}\big[\|X^n - \beta(Q(\alpha X^n) - s\boldsymbol{u})\|^2\big] \leq \frac{1}{1 - 4\epsilon_z} S_2. \tag{147}$$

We focus on the S_2 term. As before, let $\mathcal{E} := \{Q(\alpha\tilde{\boldsymbol{x}}) \neq \boldsymbol{y}\}$ be the "error" event. Then

$$S_2 = \frac{1}{n} \mathbb{E}\big[\|\tilde{\boldsymbol{x}} - \beta(Q(\alpha\tilde{\boldsymbol{x}}) - s\boldsymbol{u})\|^2 \mathbb{1}\{\mathcal{E}^{\complement}\}\big] + \frac{1}{n} \mathbb{E}\big[\|\tilde{\boldsymbol{x}} - \beta(Q(\alpha\tilde{\boldsymbol{x}}) - s\boldsymbol{u})\|^2 \mathbb{1}\{\mathcal{E}\}\big] \tag{148}$$

$$\leq \frac{1}{n} \mathbb{E}\big[\|\tilde{\boldsymbol{x}} - \beta(Q(\alpha\tilde{\boldsymbol{x}}) - s\boldsymbol{u})\|^2 \mathbb{1}\{\mathcal{E}^{\complement}\}\big] + \frac{1}{n}\sqrt{\mathbb{E}[\|\tilde{\boldsymbol{x}} - \beta(Q(\alpha\tilde{\boldsymbol{x}}) - s\boldsymbol{u})\|^4]\,\mathbb{P}(\mathcal{E})}, \tag{149}$$

where we use Cauchy-Schwarz. Note that the term with the 4-th moment satisfies

$$\mathbb{E}\big[\|\tilde{\boldsymbol{x}} - \beta(Q(\alpha\tilde{\boldsymbol{x}}) - s\boldsymbol{u})\|^4\big] \tag{150}$$

$$\leq 8(1 - \beta\alpha)\,\mathbb{E}\big[\|\tilde{\boldsymbol{x}}\|^4\big] + 8\beta\,\mathbb{E}\big[\|Q(\alpha\tilde{\boldsymbol{x}}) - \alpha\tilde{\boldsymbol{x}}\|^4\big] + 8\beta\,\mathbb{E}\big[\|s\boldsymbol{u}\|^4\big]. \tag{151}$$

The second term is $O(n^2)$ by following (136), and the third term satisfies

$$8\beta\,\mathbb{E}\big[\|s\boldsymbol{u}\|^4\big] \leq 8\beta s^4 r_{\mathrm{cov}}^4(\Lambda^{(n)}) = O(n^2) \tag{152}$$

by Lemma D.3. For the first term,

$$\mathbb{E}[\|\tilde{\boldsymbol{x}}\|^4] = \mathbb{E}\big[\|\boldsymbol{y} + \boldsymbol{z}\|^4\big] \tag{153}$$

$$\leq \mathbb{E}[\|\boldsymbol{y}\|^4] + \mathbb{E}[\|\boldsymbol{z}\|^4] + 6\,\mathbb{E}[\|\boldsymbol{y}\|^2]\,\mathbb{E}[\|\boldsymbol{z}\|^2] \tag{154}$$

$$\leq 3(\sigma^2 - \nu)^2 n + \nu^2 n(n + 2) + 6(\sigma^2 - \nu)\nu n^2 \tag{155}$$

$$= O(n^2) \tag{156}$$

for n sufficiently large, by the independence of $\boldsymbol{y}$ and $\boldsymbol{z}$, and using 4th moment results on lattice Gaussians from Zhao and Qian (2024); Micciancio and Regev (2004). Since $\lim_{n\to\infty} \mathbb{P}(\mathcal{E}) = 0$, we have that $\frac{1}{n}\sqrt{\mathbb{E}[\|\tilde{\boldsymbol{x}} - \beta(Q(\alpha\tilde{\boldsymbol{x}}) - s\boldsymbol{u})\|^4]\,\mathbb{P}(\mathcal{E})} < \frac{\epsilon}{2}$ for n sufficiently large. Thus

$$S_2 \leq \frac{1}{n} \mathbb{E}\big[\|\tilde{\boldsymbol{x}} - \beta(Q(\alpha\tilde{\boldsymbol{x}}) - s\boldsymbol{u})\|^2 \mathbb{1}\{\mathcal{E}^{\complement}\}\big] + \frac{\epsilon}{2} \tag{157}$$

$$= \mathbb{E}\left[\frac{1}{n}\|\tilde{\boldsymbol{x}} - \beta(\boldsymbol{y} - s\boldsymbol{u})\|^2 \mathbb{1}\{\mathcal{E}^{\complement}\}\right] + \frac{\epsilon}{2} \tag{158}$$

$$\leq \mathbb{E}\left[\frac{1}{n}\|\tilde{\boldsymbol{x}} - \beta(\boldsymbol{y} - s\boldsymbol{u})\|^2\right]\|\mathbb{1}\{\mathcal{E}^{\complement}\}\|_\infty + \frac{\epsilon}{2} \tag{159}$$

$$= \frac{1}{n} \mathbb{E}\big[\|\tilde{\boldsymbol{x}} - \beta(\boldsymbol{y} - s\boldsymbol{u})\|^2\big] + \frac{\epsilon}{2} \tag{160}$$

$$= \frac{1}{n} \mathbb{E}\big[\|(1 - \beta)\boldsymbol{y} + \boldsymbol{z} - \beta s\boldsymbol{u}\|^2\big] + \frac{\epsilon}{2} \tag{161}$$

$$= (1 - \beta)^2 \frac{1}{n} \mathbb{E}[\|\boldsymbol{y}\|^2] + \frac{1}{n} \mathbb{E}[\|\boldsymbol{z}\|^2] + s^2\beta^2 \frac{1}{n} \mathbb{E}[\|\boldsymbol{u}\|^2] + \frac{\epsilon}{2} \tag{162}$$

$$\leq (1 - \beta)^2(\sigma^2 - \nu) + \nu + s^2\beta^2 \cdot G(\Lambda^{(n)}) \cdot 2\pi e \cdot \frac{(\sigma^2 - \nu)\nu}{\sigma^2}(1 + \epsilon_2) + \frac{\epsilon}{2} \tag{163}$$

$$= (1 - \beta)^2(\sigma^2 - \nu) + \nu + s^2\beta^2 \frac{(\sigma^2 - \nu)\nu}{\sigma^2} + \epsilon, \tag{164}$$

for n sufficiently large, where (159) is by Hölder's inequality, and (163) holds by Banaszczyk (1993), and since the lattice second moment satisfies $\frac{1}{n}\mathbb{E}[\|\boldsymbol{u}\|^2] = G(\Lambda^{(n)}) \cdot V(\Lambda^{(n)})^{2/n}$, and the lattice sequence is quantization-good (i.e., sphere-bound-achieving). The result follows by combining (147) and (164).

27

Finally, we address the rate term. We have

$$\frac{1}{n}H(Q(\alpha X^n)) = \frac{1}{n}\mathbb{E}_{X^n}\big[-\log dP_{Q(\alpha X^n)}\big] \tag{165}$$

$$= \underbrace{\frac{1}{n}\int -\log\big(dP_{Q(\alpha\boldsymbol{x})}\big)(dP_{X^n}(\boldsymbol{x}) - dP_{\tilde{\boldsymbol{x}}}(\boldsymbol{x}))d\boldsymbol{x}}_{R_1} + \underbrace{\frac{1}{n}\mathbb{E}_{\tilde{\boldsymbol{x}}}\big[-\log dP_{Q(\alpha\tilde{\boldsymbol{x}})}\big]}_{R_2}. \tag{166}$$

The first term R_1 will vanish as $n \to \infty$, due to the following. By Regev (2009, Claim 3.9) and Ling and Belfiore (2014, Lemma 9), we have that $|dP_{\tilde{\boldsymbol{x}}}(\boldsymbol{x}) - dP_{X^n}(\boldsymbol{x})| \leq 4\epsilon_z dP_{X^n}(\boldsymbol{x}), \forall \boldsymbol{x}$, by the choice of the lattice sequence $\Lambda^{(n)}$, for n sufficiently large. Therefore,

$$R_1 \leq \frac{1}{n}\int -\log dP_{Q(\alpha\boldsymbol{x})}|dP_{X^n}(\boldsymbol{x}) - dP_{\tilde{\boldsymbol{x}}}(\boldsymbol{x})|d\boldsymbol{x} \tag{167}$$

$$\leq 4\epsilon_z \frac{1}{n}\int -\log(dP_{Q(\alpha\boldsymbol{x})})dP_{X^n}(\boldsymbol{x})d\boldsymbol{x} \tag{168}$$

$$= 4\epsilon_z \frac{1}{n}H(Q(\alpha X^n)), \tag{169}$$

which implies that

$$\frac{1}{n}H(Q(\alpha X^n)) \leq \frac{1}{1-4\epsilon_z}R_2, \tag{170}$$

for n sufficiently large.

For R_2, this is the per-dimension entropy of $Q(\alpha\tilde{\boldsymbol{x}})$. Let $p(\boldsymbol{\lambda}) := \Pr(Q(\alpha\tilde{\boldsymbol{x}}) = \boldsymbol{\lambda})$ be the PMF of $Q(\alpha\tilde{\boldsymbol{x}})$ supported on $\boldsymbol{\lambda} \in \Lambda$, and let $q_{\boldsymbol{y}}(\boldsymbol{\lambda})$ be the lattice Gaussian PMF of $\boldsymbol{y} \sim \mathcal{N}_\Lambda(\boldsymbol{0}, \sigma^2 - \nu)$. Then

$$H(Q(\alpha\tilde{\boldsymbol{x}})) = -\sum_{\boldsymbol{\lambda}\in\Lambda} p(\boldsymbol{\lambda})\log p(\boldsymbol{\lambda}) \tag{171}$$

$$\leq -\sum_{\boldsymbol{\lambda}\in\Lambda} p(\boldsymbol{\lambda})\log q_{\boldsymbol{y}}(\boldsymbol{\lambda}) \tag{172}$$

$$= \sum_{\boldsymbol{\lambda}\in\Lambda} p(\boldsymbol{\lambda})\left[\frac{1}{2(\sigma^2-\nu)}\|\boldsymbol{\lambda}\|^2 + \log\rho_{\sqrt{\sigma^2-\nu}}(\Lambda)\right] \tag{173}$$

$$= \frac{1}{2(\sigma^2-\nu)}\mathbb{E}\big[\|Q(\alpha\tilde{\boldsymbol{x}})\|^2\big] + \log\rho_{\sqrt{\sigma^2-\nu}}(\Lambda). \tag{174}$$

Combining, we have that

$$R_2 = \frac{1}{n}H(Q(\alpha\tilde{\boldsymbol{x}})) \tag{175}$$

$$\leq \frac{1}{2(\sigma^2-\nu)}\frac{1}{n}\mathbb{E}\big[\|Q(\alpha\tilde{\boldsymbol{x}})\|^2\big] + \frac{1}{n}\log\rho_{\sqrt{\sigma^2-\nu}}(\Lambda) \tag{176}$$

$$\leq \frac{1}{2(\sigma^2-\nu)}\left[\frac{1}{n}\mathbb{E}\|\boldsymbol{y}\|^2 + 2\epsilon(\sigma^2-\nu)\right] + \frac{1}{n}\log\rho_{\sqrt{\sigma^2-\nu}}(\Lambda) \tag{177}$$

$$= \frac{1}{2(\sigma^2-\nu)}\frac{1}{n}\mathbb{E}\big[\|\boldsymbol{y}\|^2\big] + \frac{1}{n}\log\rho_{\sqrt{\sigma^2-\nu}}(\Lambda) + \epsilon \tag{178}$$

$$= -\frac{1}{n}\sum_{\boldsymbol{\lambda}\in\Lambda} q_{\boldsymbol{y}}(\boldsymbol{\lambda})\log q_{\boldsymbol{y}}(\boldsymbol{\lambda}) + \epsilon \tag{179}$$

$$= \frac{1}{n}H(\boldsymbol{y}) + \epsilon, \tag{180}$$

28

for n sufficiently large, where (177) is by Lemma D.4. Therefore, for n sufficiently large, we have

$$\frac{1}{n}H(Q(\alpha X^n)) = \frac{1}{1-4\epsilon_z}\left[\frac{1}{n}H(\boldsymbol{y}) + \epsilon\right] \tag{181}$$

$$\leq \frac{1}{1-4\epsilon_z}\left[\frac{1}{2}\log\frac{\sigma^2}{\nu(1+\epsilon_2)} + \epsilon_h + \epsilon\right] \tag{182}$$

$$\leq \frac{1}{1-4\epsilon_z}\left[\frac{1}{2}\log\frac{\sigma^2}{\nu} + \epsilon_h + \epsilon\right] \tag{183}$$

where (181) is due to (170) and (180). (182) holds by Ling and Belfiore (2014, Lemma 6), the choice of volume, for n sufficiently large.

$\square$

We now prove Thm. 4.5, which is restated below.

Theorem D.6 (Optimality of PD-LTC for Gaussian sources (Thm. 4.5 in main text)). *Let* $X_1, X_2, \ldots \overset{\text{i.i.d.}}{\sim} \mathcal{N}(0, \sigma^2)$. *For any D satisfying $0 < D \leq 2\sigma^2$, there exists a sequence of PD-LTCs* $\{(g_a^{(n)}, g_s^{(n)}, \Lambda^{(n)})\}_{n=1}^{\infty}$ *such that*

$$\lim_{n\to\infty}\frac{1}{n}H(Q_{\Lambda^{(n)}}(g_a^{(n)}(X^n))) \leq R(D/2, \infty), \tag{184}$$

$$\lim_{n\to\infty}\frac{1}{n}\mathbb{E}[\|X^n - \hat{X}^n\|^2] \leq D, \tag{185}$$

$$\lim_{n\to\infty}\frac{1}{n}W_2^2(P_{X^n}, P_{\hat{X}^n}) = 0, \tag{186}$$

where $\hat{X}^n = g_s^{(n)}(Q_{\Lambda^{(n)}}(g_a^{(n)}(X^n)) + s\boldsymbol{u})$, $\boldsymbol{u} \sim \text{Unif}(\mathcal{V}(\Lambda^{(n)}))$, *and* $s = \frac{\sigma}{\sqrt{\sigma^2 - D/2}}$.

Proof. Set $s = \frac{\sigma}{\sqrt{\sigma^2 - \nu}}$, $\beta = 1$, and $\nu = \frac{D}{2}$, which satisfies (88). Choose the lattices $\Lambda^{(n)}$ as polar lattices (Liu et al., 2021; 2024). By the choice of s, $\epsilon_u = \epsilon_z = \epsilon_{\Lambda^{(n)}}\left(\sqrt{\frac{(\sigma^2-\nu)\nu}{\sigma^2}}\right)$, and therefore both flatness factors will vanish exponentially fast as $n \to \infty$ by Liu et al. (2021, Prop. 1). Additionally, by using the fact that $\epsilon_1 \leq \epsilon_{\Lambda^{(n)}}\left(\sqrt{\frac{(\sigma^2-\nu)\nu}{\sigma^2}}/\sqrt{\frac{\pi}{\pi-t}}\right)$, and since ϵ_z vanishes, taking $t \to 0$ results in a vanishing ϵ_1 and therefore vanishing ϵ_h; see Ling and Belfiore (2014, Sec. III). By Liu et al. (2019), polar lattices are AWGN-good and have exponentially decaying MAP error probability for the $\tilde{\boldsymbol{x}} = \boldsymbol{y} + \boldsymbol{z}$ AWGN channel with lattice Gaussian input, at any signal-to-noise ratio (and therefore any $\nu \in (0, \sigma^2)$). By Liu et al. (2024), the polar lattices are also quantization-good. Therefore, by Lemma D.5 we have that the rate, distortion, and perception satisfy

$$\lim_{n\to\infty}\frac{1}{n}H(Q_{\Lambda^{(n)}}(g_a^{(n)}(X^n))) \leq \frac{1}{2}\log\frac{2\sigma^2}{D}, \tag{187}$$

$$\lim_{n\to\infty}\frac{1}{n}\mathbb{E}[\|X^n - \hat{X}^n\|^2] \leq D, \tag{188}$$

$$\lim_{n\to\infty}\frac{1}{n}W_2^2(P_{X^n}, P_{\hat{X}^n}) = 0, \tag{189}$$

when the transforms are chosen to be $g_a^{(n)}(\boldsymbol{v}) = \alpha\boldsymbol{v}$ and $g_s^{(n)}(\boldsymbol{v}) = \beta\boldsymbol{v}$. $\square$

Remark D.7. In the proof of Lemma D.5 (and therefore Thm. 4.5), the condition in (88) ensures that the distribution of $\hat{X}^n$ is approximately Gaussian with covariance $\sigma^2 I_n$, and the closeness of this approximation is quantified by ϵ_u. This essentially controls how well the perception constraint can be enforced, which is why s shows up in the flatness factor. One can see that s needs to be sufficiently large to ensure $\epsilon_u = \epsilon_z$ which guarantees ϵ_u vanishes by Liu et al. (2021, Prop. 1). If s is too small, $\epsilon_u > \epsilon_z$ and it is not guaranteed it will vanish. We see that the choice of $s = \frac{\sigma}{\sqrt{\sigma^2 - D/2}} > 1$ indicates a dither $s\boldsymbol{u}$ that "bleeds" outside the lattice cell at low rates is sufficient to ensure a vanishing ϵ_u and therefore vanishing perception. This seems to imply it is not possible to choose a smaller s than

the one chosen and still make ϵ_u vanish; if this were possible, it would imply that a near-perfect perception rate-distortion tradeoff below $R(D/2, \infty)$ is achievable, which would contradict results in the RDP literature that $R(D/2, \infty)$ is the lower bound (Yan et al., 2021; Wagner, 2022; Chen et al., 2022).

On the other hand, ϵ_z is used to approximate $P_{X^n} \approx P_{\tilde{x}}$, and ϵ_h is used to approximate the entropy rate of y; as shown in the proof, a vanishing ϵ_z implies a vanishing ϵ_h.

Remark D.8. The sequence of PD-LTCs in Thm. 4.5 that satisfy the near-perfect perception constraint in (16) can be upgraded to a sequence of codes satisfying a perfect perception constraint of $P_{X^n} = P_{\hat{X}^n}$ with the same asymptotic rate and distortion, by following the "coupling argument" of Saldi et al. (2015). That is, if $\pi_{X^n, \hat{X}^n}$ is the coupling that satisfies $\frac{1}{n} W_2^2(P_{X^n}, P_{\hat{X}^n}) = \epsilon$, then one can use $\bar{X}^n \sim \pi_{X^n | \hat{X}^n}$ as the reconstruction instead of $\hat{X}^n$. This would ensure $P_{\bar{X}^n} = P_{X^n}$ and the distortion $\frac{1}{n} \mathbb{E}[\|X^n - \bar{X}^n\|^2] \leq \frac{1}{n} \mathbb{E}[\|X^n - \hat{X}^n\|^2] + \epsilon$. Since this change only affects the decoder, the rate remains the same as before.

Remark D.9. The choice of polar lattices in the proof of Thm. 4.5 may not be necessary, and other lattice families may also work. The essential requirements are that both ϵ_u and ϵ_z vanish, AWGN-goodness, quantization-goodness, and vanishing MAP error probability for the $\tilde{x} = y + z$ AWGN channel. While the latter three can be simultaneously satisfied by other lattice families, such as the mod-p lattices (Loeliger, 1997), to the best of the authors' knowledge, the only currently known lattice family with known results on vanishing ϵ_u and ϵ_z is the polar lattice. This does not preclude the existence of other lattice families that may satisfy all the aforementioned requirements.

E   Empirical Evaluation of Sliced Wasserstein

Here, we assess how accurate we can estimate the squared 2-Wasserstein Distance $W_2^2(P, Q)$ with the sliced Wasserstein distance $\mathsf{SW}_2^2(P, Q)$ (Bonneel et al., 2015). Let $P = \mathcal{N}(\mathbf{1}, I_n)$, and $Q = \mathcal{N}(\mathbf{0}, 2I_n)$. Then $\frac{1}{n} W_2^2(P, Q) = 2$. Shown in Table 2, 1, sliced Wasserstein provides fairly accurate estimate of the true Wasserstein for Gaussian samples, where N is the number of samples. This supports the use of sliced Wasserstein as a proxy for the Wasserstein distance in our experiment surrounding the Gaussian source (as we would expect the reconstruction distribution to be near-Gaussian). Therefore, the theoretical bounds are a meaningful comparison, as they align with the operational quantities of the corresponding coding theorem.

	N	Estimate	Std. Error
	100	2.129	0.282
$n = 8$	1000	1.999	0.187
	5000	2.004	0.158
	10000	1.994	0.164
	100	2.118	0.235
	1000	2.017	0.192
$n = 24$	5000	2.005	0.188
	10000	2.008	0.184

Table 1: Estimating W_2^2 using Sliced-Wasserstein with 50 projections.

	N	Estimate	Std. Error
	100	2.142	0.329
$n = 8$	1000	1.987	0.299
	5000	1.999	0.274
	10000	2.009	0.276

Table 2: Estimating W_2^2 using Sliced-Wasserstein with 20 projections.

NeurIPS Paper Checklist

1. **Claims**

   Question: Do the main claims made in the abstract and introduction accurately reflect the paper's contributions and scope?

   Answer: [Yes]

   Justification: The abstract and introduction outline the contributions of the paper and the exact sections those contributions can be found.

   Guidelines:

   - The answer NA means that the abstract and introduction do not include the claims made in the paper.
   - The abstract and/or introduction should clearly state the claims made, including the contributions made in the paper and important assumptions and limitations. A No or NA answer to this question will not be perceived well by the reviewers.
   - The claims made should match theoretical and experimental results, and reflect how much the results can be expected to generalize to other settings.
   - It is fine to include aspirational goals as motivation as long as it is clear that these goals are not attained by the paper.

2. **Limitations**

   Question: Does the paper discuss the limitations of the work performed by the authors?

   Answer: [Yes]

   Justification: The conclusion and limitations section discusses the limitations of work and what future work could address. Assumptions in our two theorems are stated in the theorem statement.

   Guidelines:

   - The answer NA means that the paper has no limitation while the answer No means that the paper has limitations, but those are not discussed in the paper.
   - The authors are encouraged to create a separate "Limitations" section in their paper.
   - The paper should point out any strong assumptions and how robust the results are to violations of these assumptions (e.g., independence assumptions, noiseless settings, model well-specification, asymptotic approximations only holding locally). The authors should reflect on how these assumptions might be violated in practice and what the implications would be.
   - The authors should reflect on the scope of the claims made, e.g., if the approach was only tested on a few datasets or with a few runs. In general, empirical results often depend on implicit assumptions, which should be articulated.
   - The authors should reflect on the factors that influence the performance of the approach. For example, a facial recognition algorithm may perform poorly when image resolution is low or images are taken in low lighting. Or a speech-to-text system might not be used reliably to provide closed captions for online lectures because it fails to handle technical jargon.
   - The authors should discuss the computational efficiency of the proposed algorithms and how they scale with dataset size.
   - If applicable, the authors should discuss possible limitations of their approach to address problems of privacy and fairness.
   - While the authors might fear that complete honesty about limitations might be used by reviewers as grounds for rejection, a worse outcome might be that reviewers discover limitations that aren't acknowledged in the paper. The authors should use their best judgment and recognize that individual actions in favor of transparency play an important role in developing norms that preserve the integrity of the community. Reviewers will be specifically instructed to not penalize honesty concerning limitations.

3. **Theory assumptions and proofs**

   Question: For each theoretical result, does the paper provide the full set of assumptions and a complete (and correct) proof?

Answer: [Yes]

Justification: The full proofs for all theoretical results can be found in Appendix. D. Furthermore, a high-level sketch of how the proofs work are discussed in the main text.

Guidelines:

- The answer NA means that the paper does not include theoretical results.
- All the theorems, formulas, and proofs in the paper should be numbered and cross-referenced.
- All assumptions should be clearly stated or referenced in the statement of any theorems.
- The proofs can either appear in the main paper or the supplemental material, but if they appear in the supplemental material, the authors are encouraged to provide a short proof sketch to provide intuition.
- Inversely, any informal proof provided in the core of the paper should be complemented by formal proofs provided in appendix or supplemental material.
- Theorems and Lemmas that the proof relies upon should be properly referenced.

4. **Experimental result reproducibility**

Question: Does the paper fully disclose all the information needed to reproduce the main experimental results of the paper to the extent that it affects the main claims and/or conclusions of the paper (regardless of whether the code and data are provided or not)?

Answer: [Yes]

Justification: The experiments section details the exact architectures and training methods (also discussed in Section 3) that can be used to reproduce the result. The code has been made publicly available at `https://github.com/leieric/LTC-RDP`.

Guidelines:

- The answer NA means that the paper does not include experiments.
- If the paper includes experiments, a No answer to this question will not be perceived well by the reviewers: Making the paper reproducible is important, regardless of whether the code and data are provided or not.
- If the contribution is a dataset and/or model, the authors should describe the steps taken to make their results reproducible or verifiable.
- Depending on the contribution, reproducibility can be accomplished in various ways. For example, if the contribution is a novel architecture, describing the architecture fully might suffice, or if the contribution is a specific model and empirical evaluation, it may be necessary to either make it possible for others to replicate the model with the same dataset, or provide access to the model. In general. releasing code and data is often one good way to accomplish this, but reproducibility can also be provided via detailed instructions for how to replicate the results, access to a hosted model (e.g., in the case of a large language model), releasing of a model checkpoint, or other means that are appropriate to the research performed.
- While NeurIPS does not require releasing code, the conference does require all submissions to provide some reasonable avenue for reproducibility, which may depend on the nature of the contribution. For example
  (a) If the contribution is primarily a new algorithm, the paper should make it clear how to reproduce that algorithm.
  (b) If the contribution is primarily a new model architecture, the paper should describe the architecture clearly and fully.
  (c) If the contribution is a new model (e.g., a large language model), then there should either be a way to access this model for reproducing the results or a way to reproduce the model (e.g., with an open-source dataset or instructions for how to construct the dataset).
  (d) We recognize that reproducibility may be tricky in some cases, in which case authors are welcome to describe the particular way they provide for reproducibility. In the case of closed-source models, it may be that access to the model is limited in some way (e.g., to registered users), but it should be possible for other researchers to have some path to reproducing or verifying the results.

5. **Open access to data and code**

   Question: Does the paper provide open access to the data and code, with sufficient instructions to faithfully reproduce the main experimental results, as described in supplemental material?

   Answer: [Yes]

   Justification: The data used is all open source and publicly available. The code has been made publicly available at `https://github.com/leieric/LTC-RDP`.

   Guidelines:

   - The answer NA means that paper does not include experiments requiring code.
   - Please see the NeurIPS code and data submission guidelines (`https://nips.cc/public/guides/CodeSubmissionPolicy`) for more details.
   - While we encourage the release of code and data, we understand that this might not be possible, so "No" is an acceptable answer. Papers cannot be rejected simply for not including code, unless this is central to the contribution (e.g., for a new open-source benchmark).
   - The instructions should contain the exact command and environment needed to run to reproduce the results. See the NeurIPS code and data submission guidelines (`https://nips.cc/public/guides/CodeSubmissionPolicy`) for more details.
   - The authors should provide instructions on data access and preparation, including how to access the raw data, preprocessed data, intermediate data, and generated data, etc.
   - The authors should provide scripts to reproduce all experimental results for the new proposed method and baselines. If only a subset of experiments are reproducible, they should state which ones are omitted from the script and why.
   - At submission time, to preserve anonymity, the authors should release anonymized versions (if applicable).
   - Providing as much information as possible in supplemental material (appended to the paper) is recommended, but including URLs to data and code is permitted.

6. **Experimental setting/details**

   Question: Does the paper specify all the training and test details (e.g., data splits, hyperparameters, how they were chosen, type of optimizer, etc.) necessary to understand the results?

   Answer: [Yes]

   Justification: The results section and appendix contain all training and test details.

   Guidelines:

   - The answer NA means that the paper does not include experiments.
   - The experimental setting should be presented in the core of the paper to a level of detail that is necessary to appreciate the results and make sense of them.
   - The full details can be provided either with the code, in appendix, or as supplemental material.

7. **Experiment statistical significance**

   Question: Does the paper report error bars suitably and correctly defined or other appropriate information about the statistical significance of the experiments?

   Answer: [No]

   Justification: It is standard in the neural compression literature for the metrics to be reported as averages over the test set using the final converged model. This is the metric reporting that we follow for rate, distortion, and perception metrics.

   Guidelines:

   - The answer NA means that the paper does not include experiments.
   - The authors should answer "Yes" if the results are accompanied by error bars, confidence intervals, or statistical significance tests, at least for the experiments that support the main claims of the paper.

- The factors of variability that the error bars are capturing should be clearly stated (for example, train/test split, initialization, random drawing of some parameter, or overall run with given experimental conditions).
- The method for calculating the error bars should be explained (closed form formula, call to a library function, bootstrap, etc.)
- The assumptions made should be given (e.g., Normally distributed errors).
- It should be clear whether the error bar is the standard deviation or the standard error of the mean.
- It is OK to report 1-sigma error bars, but one should state it. The authors should preferably report a 2-sigma error bar than state that they have a 96% CI, if the hypothesis of Normality of errors is not verified.
- For asymmetric distributions, the authors should be careful not to show in tables or figures symmetric error bars that would yield results that are out of range (e.g. negative error rates).
- If error bars are reported in tables or plots, The authors should explain in the text how they were calculated and reference the corresponding figures or tables in the text.

8. **Experiments compute resources**

Question: For each experiment, does the paper provide sufficient information on the computer resources (type of compute workers, memory, time of execution) needed to reproduce the experiments?

Answer: [Yes]

Justification: The GPUs used are mentioned in the appendix.

Guidelines:

- The answer NA means that the paper does not include experiments.
- The paper should indicate the type of compute workers CPU or GPU, internal cluster, or cloud provider, including relevant memory and storage.
- The paper should provide the amount of compute required for each of the individual experimental runs as well as estimate the total compute.
- The paper should disclose whether the full research project required more compute than the experiments reported in the paper (e.g., preliminary or failed experiments that didn't make it into the paper).

9. **Code of ethics**

Question: Does the research conducted in the paper conform, in every respect, with the NeurIPS Code of Ethics https://neurips.cc/public/EthicsGuidelines?

Answer: [Yes]

Justification: The paper conforms to the code of ethics.

Guidelines:

- The answer NA means that the authors have not reviewed the NeurIPS Code of Ethics.
- If the authors answer No, they should explain the special circumstances that require a deviation from the Code of Ethics.
- The authors should make sure to preserve anonymity (e.g., if there is a special consideration due to laws or regulations in their jurisdiction).

10. **Broader impacts**

Question: Does the paper discuss both potential positive societal impacts and negative societal impacts of the work performed?

Answer: [Yes]

Justification: While there is a connection between RDP compressors and generative models, we do not expect there to be any significant adverse societal impacts of the work.

Guidelines:

- The answer NA means that there is no societal impact of the work performed.

- If the authors answer NA or No, they should explain why their work has no societal impact or why the paper does not address societal impact.
- Examples of negative societal impacts include potential malicious or unintended uses (e.g., disinformation, generating fake profiles, surveillance), fairness considerations (e.g., deployment of technologies that could make decisions that unfairly impact specific groups), privacy considerations, and security considerations.
- The conference expects that many papers will be foundational research and not tied to particular applications, let alone deployments. However, if there is a direct path to any negative applications, the authors should point it out. For example, it is legitimate to point out that an improvement in the quality of generative models could be used to generate deepfakes for disinformation. On the other hand, it is not needed to point out that a generic algorithm for optimizing neural networks could enable people to train models that generate Deepfakes faster.
- The authors should consider possible harms that could arise when the technology is being used as intended and functioning correctly, harms that could arise when the technology is being used as intended but gives incorrect results, and harms following from (intentional or unintentional) misuse of the technology.
- If there are negative societal impacts, the authors could also discuss possible mitigation strategies (e.g., gated release of models, providing defenses in addition to attacks, mechanisms for monitoring misuse, mechanisms to monitor how a system learns from feedback over time, improving the efficiency and accessibility of ML).

11. **Safeguards**

Question: Does the paper describe safeguards that have been put in place for responsible release of data or models that have a high risk for misuse (e.g., pretrained language models, image generators, or scraped datasets)?

Answer: [NA]

Justification: The work does not release such data or models.

Guidelines:

- The answer NA means that the paper poses no such risks.
- Released models that have a high risk for misuse or dual-use should be released with necessary safeguards to allow for controlled use of the model, for example by requiring that users adhere to usage guidelines or restrictions to access the model or implementing safety filters.
- Datasets that have been scraped from the Internet could pose safety risks. The authors should describe how they avoided releasing unsafe images.
- We recognize that providing effective safeguards is challenging, and many papers do not require this, but we encourage authors to take this into account and make a best faith effort.

12. **Licenses for existing assets**

Question: Are the creators or original owners of assets (e.g., code, data, models), used in the paper, properly credited and are the license and terms of use explicitly mentioned and properly respected?

Answer: [NA]

Justification: The paper does not use existing assets.

Guidelines:

- The answer NA means that the paper does not use existing assets.
- The authors should cite the original paper that produced the code package or dataset.
- The authors should state which version of the asset is used and, if possible, include a URL.
- The name of the license (e.g., CC-BY 4.0) should be included for each asset.
- For scraped data from a particular source (e.g., website), the copyright and terms of service of that source should be provided.

- If assets are released, the license, copyright information, and terms of use in the package should be provided. For popular datasets, paperswithcode.com/datasets has curated licenses for some datasets. Their licensing guide can help determine the license of a dataset.
- For existing datasets that are re-packaged, both the original license and the license of the derived asset (if it has changed) should be provided.
- If this information is not available online, the authors are encouraged to reach out to the asset's creators.

13. **New assets**

    Question: Are new assets introduced in the paper well documented and is the documentation provided alongside the assets?

    Answer: [NA]

    Justification: The paper does not release new assets.

    Guidelines:

    - The answer NA means that the paper does not release new assets.
    - Researchers should communicate the details of the dataset/code/model as part of their submissions via structured templates. This includes details about training, license, limitations, etc.
    - The paper should discuss whether and how consent was obtained from people whose asset is used.
    - At submission time, remember to anonymize your assets (if applicable). You can either create an anonymized URL or include an anonymized zip file.

14. **Crowdsourcing and research with human subjects**

    Question: For crowdsourcing experiments and research with human subjects, does the paper include the full text of instructions given to participants and screenshots, if applicable, as well as details about compensation (if any)?

    Answer: [NA]

    Justification: The paper does not involve crowdsourcing nor research with human subjects.

    Guidelines:

    - The answer NA means that the paper does not involve crowdsourcing nor research with human subjects.
    - Including this information in the supplemental material is fine, but if the main contribution of the paper involves human subjects, then as much detail as possible should be included in the main paper.
    - According to the NeurIPS Code of Ethics, workers involved in data collection, curation, or other labor should be paid at least the minimum wage in the country of the data collector.

15. **Institutional review board (IRB) approvals or equivalent for research with human subjects**

    Question: Does the paper describe potential risks incurred by study participants, whether such risks were disclosed to the subjects, and whether Institutional Review Board (IRB) approvals (or an equivalent approval/review based on the requirements of your country or institution) were obtained?

    Answer: [NA]

    Justification: The paper does not involve crowdsourcing nor research with human subjects.

    Guidelines:

    - The answer NA means that the paper does not involve crowdsourcing nor research with human subjects.
    - Depending on the country in which research is conducted, IRB approval (or equivalent) may be required for any human subjects research. If you obtained IRB approval, you should clearly state this in the paper.

- We recognize that the procedures for this may vary significantly between institutions and locations, and we expect authors to adhere to the NeurIPS Code of Ethics and the guidelines for their institution.
- For initial submissions, do not include any information that would break anonymity (if applicable), such as the institution conducting the review.

16. **Declaration of LLM usage**

    Question: Does the paper describe the usage of LLMs if it is an important, original, or non-standard component of the core methods in this research? Note that if the LLM is used only for writing, editing, or formatting purposes and does not impact the core methodology, scientific rigorousness, or originality of the research, declaration is not required.

    Answer: [NA]

    Justification: The core method development in this research does not involve LLMs as any important, original, or non-standard components.

    Guidelines:

    - The answer NA means that the core method development in this research does not involve LLMs as any important, original, or non-standard components.
    - Please refer to our LLM policy (https://neurips.cc/Conferences/2025/LLM) for what should or should not be described.